The Journal of Chemical Physics ARTICLE scitation.org/journal/jcp

Relativistic study of parity-violating nuclear spin-rotation tensors

Cite as: J. Chem. Phys. 155, 134307 (2021); doi: 10.1063/5.0065487
Submitted: 2 August 2021 • Accepted: 16 September 2021 •
Published Online: 7 October 2021

Ignacio Agustín Aucar[1,a] and Anastasia Borschevsky[2,b]

AFFILIATIONS

[1] Instituto de Modelado e Innovación Tecnológica (UNNE-CONICET), Facultad de Ciencias Exactas y Naturales y Agrimensura, Universidad Nacional del Nordeste, Avda. Libertad, 5460 Corrientes, Argentina

[2] Faculty of Science and Engineering, Van Swinderen Institute for Particle Physics and Gravity, University of Groningen, 9747 AG Groningen, The Netherlands

[a] **Author to whom correspondence should be addressed:** agustin.aucar@conicet.gov.ar
[b] **Electronic mail:** a.borschevsky@rug.nl

ABSTRACT

We present a four-component relativistic approach to describe the effects of the nuclear spin-dependent parity-violating (PV) weak nuclear forces on nuclear spin-rotation (NSR) tensors. The formalism is derived within the four-component polarization propagator theory based on the Dirac–Coulomb Hamiltonian. Such calculations are important for planning and interpretation of possible future experiments aimed at stringent tests of the standard model through the observation of PV effects in NSR spectroscopy. An exploratory application of this theory to the chiral molecules H_2X_2 ($X = {}^{17}O$, ${}^{33}S$, ${}^{77}Se$, ${}^{125}Te$, and ${}^{209}Po$) illustrates the dramatic effect of relativity on these contributions. In particular, spin-free and spin–orbit effects are even of opposite signs for some dihedral angles, and the latter fully dominate for the heavier nuclei. Relativistic four-component calculations of isotropic nuclear spin-rotation constants, including parity-violating electroweak interactions, give frequency differences of up to 4.2 mHz between the H_2Po_2 enantiomers; on the nonrelativistic level of theory, this energy difference is 0.1 mHz only.

I. INTRODUCTION

Parity non-conservation was postulated in weak interactions by Lee and Yang[1] and first verified experimentally by Wu *et al.*[2] The parity non-conservation law states that the mirror symmetry of nature, i.e., the symmetry regarding inversion of the coordinates of all particles in a system, is broken down for physical phenomena due to the weak interactions, which are responsible for the nuclear β-decay.

When the parity non-conservation law is applied to molecular systems, the electromagnetic forces play an important role as well. Electroweak theory states that the exchange of Z^0 bosons between electrons and nuclei should cause an electronic energy splitting for the two enantiomers of a chiral molecule due to parity-violating (PV) effects.[3,4] While the exchange of Z^0 bosons between (stable) nuclei and electrons in a molecule is expected to dominate the appearing PV effects,[5] the exchange of the $W^{\pm}$ bosons is also important for describing such effects. In particular, it is responsible for the PV interactions between nucleons, which give rise to a nuclear anapole moment that is coupled to the electrons by means of electromagnetic interactions. In addition, the exchange of the weak interaction Z^0 and $W^{\pm}$ particles plays an important role in molecules containing nuclei subject to β-decays.

The interest in experimental investigations of PV effects increased after the work of Bouchiat and Bouchiat, who pointed out that a considerable enhancement of sensitivity to these effects should be expected for heavy atoms.[6] Atomic parity violation was detected in Cs in 1997;[7] other experiments focused on atoms such as Tl, Pb, Bi, and Yb.[7–13] In the case of chiral molecules, an energy splitting is expected to be found between the two enantiomers due to PV interactions.[5]

Currently, experimental searches for PV effects in chiral molecules involve resonance frequency splittings in the rotational, vibrational, and electronic spectroscopies,[4,14–17] as well as studies of their influence on nuclear magnetic resonance (NMR) parameters such as shieldings or spin–spin coupling tensors.[18–28] In spite of the

ever-improving precision of such experiments, PV effects in chiral molecules have not yet been detected.

In this work, we focus our attention on the role of parity-violating nuclear spin-rotation (PV-NSR) tensors. To our knowledge, Barra, Robert, and Wiesenfeld were the first to publish a nonrelativistic (NR) formulation of the PV-NSR tensors.[19]

Recently, we have derived a theoretical formalism and applied it to molecular calculations, demonstrating that relativistic effects play an important role in the description of parity conserving NSR tensors.[29–31] This was later confirmed by other research groups using the same and also other theoretical derivations.[32–34]

Here, we apply the same formalism to perform the first four-component (4c) relativistic calculations of the PV effects on NSR constants. We investigate the PV-NSR tensors of the X nuclei in the H_2X_2 series of molecules (with X = ^{17}O, ^{33}S, ^{77}Se, ^{125}Te, and ^{209}Po). The selection of this class of systems for study was not motivated by their experimental potential. It is well-known that the NSR interaction is the main hyperfine effect that produces line splittings in spectra when the analyzed molecules contain nuclei with zero electric quadrupole moment. This is not the case for some of the systems under study in this work, making the disentanglement of the different effects problematic. Furthermore, the H_2X_2 series of molecules are not suitable candidates for experimental detection of PV effects because the hydrogen atoms can be placed at almost all angles around the X–X bonds (i.e., these are non-rigid structures). The reason for selection of these molecules for the present study is their simple structure and the fact that they were extensively used in the past to investigate the influence of PV effects on molecular properties within various theoretical frameworks.[23,25–27,35–37] Therefore, they are well suited to be considered as test systems for the first investigation of PV effects on NSR tensors within a 4c relativistic approach.

In this work, we report a systematic study of relativistic and electronic correlation effects on the PV contribution to the isotropic NSR constants of light and heavy nuclei in the P enantiomer of the H_2X_2 chiral molecules. We used a linear response approach within the random phase approximation (RPA) and also employed density functional theory (DFT). The Dirac–Coulomb Hamiltonian was used, and we also compare our 4c results with their NR limits, obtained by using the Lévy–Leblond Hamiltonian. The spin–orbit (SO) contributions are shown to be dominant for the molecules containing heavy nuclei (^{125}Te and ^{209}Po).

This paper is structured as follows: In Sec. II, we present the 4c relativistic formulation of the calculations of the PV-NSR tensors using a linear response approach. To achieve this goal, we first show the employed 4c perturbed Hamiltonian as well as its NR limit. In this way, we are in a position to compare the NR limit of our 4c theory with previous formulations of PV-NMR-shielding and PV-NSR tensors.[19–21] In Sec. III, we provide the computational details for all the calculations presented in this paper. In Sec. IV, we start by studying the basis set convergence of 4c calculations of PV-NMR-shielding and NSR constants. Then, a comparison with results published in previous works for the PV-NMR-shielding constants is introduced.[23,26,27] Finally, the first 4c computations of PV (isotropic) NSR constants are presented for the X nuclei (X = ^{17}O, ^{33}S, ^{77}Se, ^{125}Te, and ^{209}Po) of the H_2X_2 molecules. The effect of the relativistic and electronic correlation effects is also discussed in this part of the paper.

II. THEORY

In response theory, molecular properties can be calculated at different levels of approximation within wave function, density functional theory (DFT), or polarization propagator formalisms.[38–40] Within Rayleigh–Schrödinger perturbation theory, second-order corrections to the ground state electronic energy are given by

$$E^{(2)}_{PQ} = \sum_{n\neq 0} \frac{\langle 0|\hat{H}^P|n\rangle\langle n|\hat{H}^Q|0\rangle}{E_0 - E_n} + c.c., \tag{1}$$

with $c.c.$ standing for the complex conjugate of the preceding terms and $|n\rangle$ being a complete set of eigenstates of the unperturbed molecular Hamiltonian. The operators $\hat{H}^P$ and $\hat{H}^Q$ are any perturbative Hamiltonians. In addition, any static second-order molecular property can also be calculated by using polarization propagator theory as[41]

$$E^{(2)}_{PQ} = \mathrm{Re}\left[\left\langle\left\langle \hat{H}^P ; \hat{H}^Q \right\rangle\right\rangle_{\omega=0}\right], \tag{2}$$

where the linear response function at zero frequency

$$\left\langle\left\langle \hat{H}^P ; \hat{H}^Q \right\rangle\right\rangle_{\omega=0} = \mathbf{b}^P\, \mathbf{M}^{-1}\, \mathbf{b}^Q \tag{3}$$

is constructed from the property matrix elements $\mathbf{b}^P$ and $\mathbf{b}^Q$ (the perturbators, as they were named within semi-empirical models) and the principal propagator $\mathbf{M}^{-1}$.[42] As the explicit calculation of the principal propagator (which is the inverse of the electronic Hessian) is computationally too expensive, the linear response function is computed by first solving the response equation

$$\mathbf{M}\, \mathbf{X}^Q(\omega) = \mathbf{b}^Q, \tag{4}$$

where the solution vector of Eq. (4), i.e., $\mathbf{X}^Q(\omega) = \mathbf{M}^{-1}\mathbf{b}^Q$, is first expanded in trial vectors. Then, it is contracted with the property matrix $\mathbf{b}^P$.[43]

A. Parity-violating response properties

Within the relativistic framework, the PV electron–nucleus effective interaction operator corresponding to the lowest order Z^0-exchange between electrons and nuclei is given by[4,44,45]

$$\hat{H}^{PV} = \frac{G_F}{2\sqrt{2}} \sum_{i,N} Q_{w,N} \gamma^5_i \rho_N(\boldsymbol{r}_i) - \frac{G_F\left(1 - 4\sin^2\theta_W\right)}{\sqrt{2}} \sum_{i,N} \lambda_N\, \boldsymbol{\alpha}_i \cdot \boldsymbol{I}_N\, \rho_N(\boldsymbol{r}_i). \tag{5}$$

The sums with indices i and N run over all electrons and nuclei, respectively. G_F is the Fermi coupling constant, whose most recent value is $G_F/(\hbar\, c_0)^3 = 1.166\,378\,7 \times 10^{-5}$ GeV^{-2}, i.e., $G_F \simeq 2.222\,516 \times 10^{-14}\, E_h\, a_0^3$.[46] $Q_{w,N} = Z_N\left(1 - 4\sin^2\theta_W\right) - N_N$ is the weak nuclear charge with Z_N and N_N being the number of protons and neutrons of nucleus N, respectively. While the most recent value of the sine-squared weak mixing angle θ_W is 0.238 57(5),[47] we use $\sin^2\theta_W = 0.2319$[48] as the Weinberg parameter throughout this work for ease of comparison with earlier investigations.[23,26,27] The 4×4 γ^5_i

and $\boldsymbol{\alpha}_i$ Dirac matrices operate on spinors of electron i and are given by

$$\gamma_i^5 = \begin{pmatrix} \mathbf{0} & \mathbf{1} \\ \mathbf{1} & \mathbf{0} \end{pmatrix}, \qquad \boldsymbol{\alpha}_i = \begin{pmatrix} \mathbf{0} & \boldsymbol{\sigma}_i \\ \boldsymbol{\sigma}_i & \mathbf{0} \end{pmatrix}, \tag{6}$$

with $\mathbf{0}$, $\mathbf{1}$, and $\boldsymbol{\sigma}_i$ being the two-by-two zero, identity, and Pauli spin matrices, respectively. $\boldsymbol{r}_i$ is the position of electron i with respect to the coordinate origin, $\rho_N(\boldsymbol{r}_i)$ is the normalized electric nuclear charge density of nucleus N at the position of electron i (given in units of the inverse of cube distances), λ_N is a nuclear state dependent parameter, and $\boldsymbol{I}_N$ is the dimensionless nuclear spin operator. The SI units are adopted in the present work.

The first and second terms on the right-hand side of Eq. (5) are the nuclear spin-independent and spin-dependent one-electron contributions to the PV Hamiltonian, respectively. In this work, we do not address the spin-independent terms, and their effects will not be analyzed here. We therefore set

$$\begin{aligned} \hat{H}^{PV} &= \hat{H}^{PV}_{\mathrm{SD}} \\ &= -\frac{G_F\left(1-4\sin^2\theta_W\right)}{\sqrt{2}} \sum_{i,N} \lambda_N \, \boldsymbol{\alpha}_i \cdot \boldsymbol{I}_N \, \rho_N(\boldsymbol{r}_i). \end{aligned} \tag{7}$$

For the sake of comparison with previous works,[23,26] we have set the parameter $\lambda_N = 1$ in all of our calculations. To be able to compare our results with those obtained experimentally, the calculations have to be scaled with the actual value of λ_N, which is estimated to be of order 10^0 to 10^1 for heavy nuclei.[49] The contribution of the nuclear anapole moment was not taken into account for the calculations of the PV-NMR-shieldings and PV-NSR tensor elements.

1. Parity-violating nuclear spin-rotation tensor

The nuclear spin-rotation (NSR) tensor of a nucleus N, $\boldsymbol{M}_N$, is obtained from the energy derivative,[29,31]

$$\boldsymbol{M}_N = -\hbar \left. \frac{\partial^2 E}{\partial \boldsymbol{I}_N \partial \boldsymbol{J}} \right|_{\boldsymbol{I}_N=\boldsymbol{J}=0}, \tag{8}$$

where $\hbar = \frac{h}{2\pi}$ is the reduced Planck constant, $\boldsymbol{I}_N$ is the dimensionless spin of nucleus N, and $\boldsymbol{J}$ is the molecular rotational angular momentum around the (molecular) center of mass.

In a relativistic framework, the perturbative Hamiltonian associated with the molecular rotational angular momentum can be written [for details, see Eq. (60) of Ref. 31] as[29,50]

$$\hat{H}^{J} = -\boldsymbol{\omega} \cdot \boldsymbol{J}_e + \hat{H}^{J-Breit}, \tag{9}$$

where $\boldsymbol{\omega} = \boldsymbol{I}^{-1} \cdot \boldsymbol{L}_N$ is the molecular angular velocity, $\boldsymbol{I}^{-1}$ is the inverse molecular inertia tensor with respect to the molecular center of mass (CM) in the equilibrium geometry, and $\boldsymbol{J}_e = \boldsymbol{L}_e + \boldsymbol{S}_e$ is the 4×4 total electronic angular momentum operator. In the present work, we do not include the effects of the Breit electron–nucleus interaction $\hat{H}^{J-Breit}$ due to their very small influence with respect to its precedent term in Eq. (9).[50]

By combining Eqs. (7) and (9) with Eqs. (2) and (8), we obtain the PV contribution to the NSR tensor as the linear response function,

$$\boldsymbol{M}_N^{PV} = -\hbar \frac{G_F\left(1-4\sin^2\theta_W\right)}{\sqrt{2}\, c_0} \lambda_N \langle\langle \, \rho_N(\boldsymbol{r}) \; c\boldsymbol{\alpha} \; ; \; \boldsymbol{J}_e \, \rangle\rangle_{\omega=0} \cdot \boldsymbol{I}^{-1}, \tag{10}$$

where $\frac{1}{c_0}$ is linearly proportional to the fine structure constant (in SI units, the fine structure constant is $\frac{1}{4\pi\epsilon_0}\frac{e^2}{\hbar\, c_0}$) and c is the speed of light in vacuum, scalable to infinity at the NR limit.

2. Parity-violating NMR shielding tensor

The NMR shielding tensor of a nucleus N is the second derivative of the energy with respect to its nuclear magnetic moment, $\boldsymbol{\mu}_N$, and a uniform external magnetic field, $\boldsymbol{B}_0$, at zero frequency,

$$\boldsymbol{\sigma}_N = \left. \frac{\partial^2 E}{\partial \boldsymbol{\mu}_N \partial \boldsymbol{B}_0} \right|_{\boldsymbol{\mu}_N=\boldsymbol{B}_0=0}. \tag{11}$$

At the 4c level of theory, the perturbation Hamiltonian related with the external magnetic field is

$$\hat{H}^{\boldsymbol{B}} = -\frac{e}{2} \, \boldsymbol{B}_0 \cdot \sum_i c \, \boldsymbol{\alpha}_i \times (\boldsymbol{r}_i - \boldsymbol{R}_{GO}) \tag{12}$$

with $\boldsymbol{\mu}_N = \gamma_N \hbar \, \boldsymbol{I}_N$, where $\gamma_N = \frac{e}{2m_p} g_N$ is the gyromagnetic ratio of nucleus N and its g-factor g_N. In addition, e is the fundamental charge and $\boldsymbol{R}_{GO}$ is the gauge origin position for the external magnetic potential.

Therefore, the PV contribution to the NMR shielding tensor is given by[23,26,27]

$$\begin{aligned} \boldsymbol{\sigma}_N^{PV} = & \frac{G_F\left(1-4\sin^2\theta_W\right)}{\sqrt{2}} \, \frac{2m_p}{\hbar\, c_0} \frac{1}{g_N} \lambda_N \\ & \times \left\langle\!\!\left\langle \, \rho_N(\boldsymbol{r}) \; c\boldsymbol{\alpha} \; ; \; \frac{c}{2}\boldsymbol{\alpha} \times (\boldsymbol{r} - \boldsymbol{R}_{GO}) \, \right\rangle\!\!\right\rangle_{\omega=0}. \end{aligned} \tag{13}$$

B. NR limit of PV response properties within the LRESC model

The linear response within the elimination of small component (LRESC) model allows us to expand second order relativistic properties in terms of the fine structure constant. Within this approach, the zeroth order terms of these expansions yield the NR expressions of the properties, and their relativistic corrections are obtained by employing the elimination of the small component (ESC) approach.[51,52] This model allows us to unveil the physical mechanisms behind the relativistic effects of the analyzed properties.

The NR expressions for the PV-NMR-shielding and PV-NSR tensors are derived in this section applying the LRESC approach. As the details of this model were extensively discussed elsewhere,[29,51–53] we only focus on the main steps to yield the NR limit for the properties of interest on this work. Their leading order relativistic corrections may be also obtained employing this methodology, but this is out of the scope of the present work.

The main purpose of this section is to obtain the NR expression of the PV-NSR tensor starting from the relativistic theory derived

in Sec. II A 1. In this way, it should be confirmed that the NR limit of Eq. (10) must be equal to the expression derived by Barra and co-workers within the NR domain.[19]

1. NR limit of response properties within the LRESC model

Within the relativistic polarization propagator theory, it is well known that the 4c expressions of second-order response properties may be written as the sum two terms, one involving the positive energy spectrum of electronic states [in other words, involving only (e–e) excitations] and a second one where only excitations to negative energy electronic orbitals, i.e., virtual electron–positron pairs in the QED picture, are allowed (e-p excitations).[52]

In other words, as the off-diagonal contributions to the principal propagator $\mathbf{M}^{-1}$ of Eq. (3) are smaller than the diagonal ones,[54] the leading contributions to the linear response function will be only related to the diagonal terms, meaning that Eq. (3) can be approximated as

$$\langle\langle\, \hat{H}^P\,;\,\hat{H}^Q\,\rangle\rangle \approx \langle\langle\, \hat{H}^P\,;\,\hat{H}^Q\,\rangle\rangle^{(e-e)} + \langle\langle\, \hat{H}^P\,;\,\hat{H}^Q\,\rangle\rangle^{(p-p)}. \tag{14}$$

In the NR limit, $\langle\langle\, \hat{H}^P\,;\,\hat{H}^Q\,\rangle\rangle^{(e-e)}$ and $\langle\langle\, \hat{H}^P\,;\,\hat{H}^Q\,\rangle\rangle^{(p-p)}$ are usually the paramagnetic and diamagnetic contributions, respectively, of any response magnetic property.

In order to expand the (e–e) contributions to a linear response function within the LRESC model, we apply the ESC approach to transform the 4c matrix elements of operators $\hat{H}^P$ and $\hat{H}^Q$ to the Pauli space of spinors $\tilde{\phi}$,

$$\langle\phi_i^{(4)}|\hat{H}^P|\phi_j^{(4)}\rangle \simeq \langle\tilde{\phi}_i|\hat{O}(\hat{H}^P)|\tilde{\phi}_j\rangle. \tag{15}$$

Expanding Eq. (15), we can write the operator $\hat{O}(\hat{H}^P)$ as

$$\hat{O}(\hat{H}^P) = \hat{O}^{NR}(\hat{H}^P) + \mathscr{O}(c^{-2}), \tag{16}$$

where $\hat{O}^{NR}(\hat{H}^P)$ groups the zeroth order contributions of a series expansion in terms of c^{-2} and $\mathscr{O}(c^{-2})$ are all higher order terms.

Within this approximation, we obtain

$$\langle\langle\, \hat{H}^P\,;\,\hat{H}^Q\,\rangle\rangle^{(e-e)} = \langle\langle\, \hat{O}^{NR}(\hat{H}^P)\,;\,\hat{O}^{NR}(\hat{H}^Q)\,\rangle\rangle + \mathscr{O}(c^{-2}), \tag{17}$$

where the first term on the right-hand side of Eq. (17) is the NR limit of $\langle\langle\, \hat{H}^P\,;\,\hat{H}^Q\,\rangle\rangle^{(e-e)}$.

On the other hand, the (p–p) contribution to a linear response function can be expanded within the LRESC model, retaining only leading order relativistic terms, by calculating[52]

$$\langle\langle\, \hat{H}^P\,;\,\hat{H}^Q\,\rangle\rangle^{(p-p)} \simeq \frac{1}{2mc^2}\big[\langle\Psi_0|\hat{H}^P\hat{P}_p\hat{X}(\hat{H}^Q)|\Psi_0\rangle + \langle\Psi_0|\hat{H}^Q\hat{P}_p\hat{X}(\hat{H}^P)|\Psi_0\rangle\big], \tag{18}$$

where Ψ_0 is the 4c wave function corresponding to the ground state solution of the Dirac–Hartree–Fock (DHF) approximation and $\hat{P}_p$ is the projector onto the positronic states. When the operator $\hat{X}(\hat{H}^P)$ is expanded in a series in terms of c^{-2} and only the leading order terms are retained, it is found that[51]

$$\begin{aligned}\hat{X}(\hat{H}^P) &= 2\,\hat{H}^P + \frac{1}{2mc^2}[\hat{H}^{DCB}, \hat{H}^P] \\ &= 2\,\hat{H}^P + \frac{1}{2}[\beta, \hat{H}^P] + \mathscr{O}(c^{-1}),\end{aligned} \tag{19}$$

where $\hat{H}^{DCB}$ is the unperturbed Dirac–Coulomb–Breit molecular Hamiltonian, β is the Dirac operator, and [,] refers to the commutator between two operators.[51,52]

It can be shown that the zeroth order term of the expansion of Eq. (18) is given by[51–53]

$$\langle\langle\, \hat{H}^P\,;\,\hat{H}^Q\,\rangle\rangle^{(p-p)} = \frac{1}{2mc^2}\big[\langle\Psi_0^L|\hat{H}_{LS}^P\,\hat{X}_{SL}(\hat{H}^Q)|\Psi_0^L\rangle + \langle\Psi_0^L|\hat{H}_{LS}^Q\,\hat{X}_{SL}(\hat{H}^P)|\Psi_0^L\rangle\big] \tag{20}$$

because at this lowest order $\hat{P}_p = \begin{pmatrix} 0 & 0 \\ 0 & 1 \end{pmatrix}$ and $|\Psi_0\rangle = \begin{pmatrix} |\Psi_0^L\rangle \\ 0 \end{pmatrix}$. To derive Eq. (20), it was assumed that in the matrix representation, we can express

$$\hat{H}^P = \begin{pmatrix} \hat{H}_{LL}^P & \hat{H}_{LS}^P \\ \hat{H}_{SL}^P & \hat{H}_{SS}^P \end{pmatrix}, \quad \hat{X}(\hat{H}^P) = \begin{pmatrix} \hat{X}_{LL}(\hat{H}^P) & \hat{X}_{LS}(\hat{H}^P) \\ \hat{X}_{SL}(\hat{H}^P) & \hat{X}_{SS}(\hat{H}^P) \end{pmatrix}. \tag{21}$$

2. NR limit of the (e-e) contribution to M_N^{PV}

In the particular case of the PV-NSR tensor, the perturbative Hamiltonians are $\hat{H}^{PV}$ and $\hat{H}^J$ [see Eqs. (7) and (9)].

The 4c matrix elements of $\hat{H}^{PV}$ are

$$\langle\phi_i^{(4)}|\boldsymbol{\alpha}\cdot\boldsymbol{I}_N\,\rho_N(\boldsymbol{r})|\phi_j^{(4)}\rangle \simeq \langle\tilde{\phi}_i|\left\{\left(\frac{\boldsymbol{\sigma}\cdot\boldsymbol{p}}{2mc}\right),\,\boldsymbol{\sigma}\cdot\boldsymbol{I}_N\,\rho_N(\boldsymbol{r})\right\}|\tilde{\phi}_j\rangle + \mathscr{O}(c^{-1}), \tag{22}$$

where $\{,\}$ stands for the anticommutation of two operators.

In order to obtain Eq. (22), it was assumed that at the leading order of approximation, the large and small components of $|\phi_i^{(4)}\rangle$ are related by[51]

$$|\phi_i^S\rangle \approx \frac{1}{2mc}\boldsymbol{\sigma}\cdot\boldsymbol{p}\,|\phi_i^L\rangle, \tag{23}$$

and that at zeroth order, the "normalized" spinor $|\tilde{\phi}_i\rangle$ is equal to $|\phi_i^L\rangle$.[51]

Retaining only the leading order contribution to Eq. (22) in a series expansion in terms of c^{-1}, we obtain

$$\langle\phi_i^{(4)}|\boldsymbol{\alpha}\cdot\boldsymbol{I}_N\,\rho_N(\boldsymbol{r})|\phi_j^{(4)}\rangle \simeq \frac{1}{2mc}\langle\tilde{\phi}_i|\{\boldsymbol{\sigma}\cdot\boldsymbol{p},\,\boldsymbol{\sigma}\cdot\boldsymbol{I}_N\,\rho_N(\boldsymbol{r})\}|\tilde{\phi}_j\rangle. \tag{24}$$

By combining Eqs. (15), (16), and (24), it can be easily seen that

$$\hat{O}^{NR}(\hat{H}^{PV}) = -\frac{G_F\big(1-4\sin^2\theta_W\big)}{\sqrt{2}}\sum_{i,N}\frac{\lambda_N}{2mc}\big\{\boldsymbol{\sigma}_i\cdot\boldsymbol{p}_i\,,\,\boldsymbol{\sigma}_i\cdot\boldsymbol{I}_N\,\rho_N(\boldsymbol{r}_i)\big\}. \tag{25}$$

If the Dirac identity

$$\boldsymbol{\sigma}\cdot\boldsymbol{A}\;\boldsymbol{\sigma}\cdot\boldsymbol{B} = \boldsymbol{A}\cdot\boldsymbol{B} + i\boldsymbol{\sigma}\cdot\boldsymbol{A}\times\boldsymbol{B} \tag{26}$$

is applied to Eq. (25), then we get

$$\hat{O}^{NR}(\hat{H}^{PV}) = -\frac{G_F\left(1-4\sin^2\theta_W\right)}{\sqrt{2}}\sum_{i,N}\frac{\lambda_N}{2mc} \times \left(\boldsymbol{I}_N\cdot\left\{\boldsymbol{p}_i\,,\,\rho_N(\boldsymbol{r_i})\right\}+i\left[\boldsymbol{p}_i\,,\,\rho_N(\boldsymbol{r_i})\right]\cdot\boldsymbol{I}_N\times\boldsymbol{\sigma}_i\right). \quad (27)$$

This expression agrees with an equivalent one derived in Ref. 26 by employing another methodology.

To obtain the NR limit of the PV-NSR tensor by employing the LRESC model, the perturbed Hamiltonian of Eq. (9) should also be replaced into the left-hand side of Eq. (15). By doing so, we obtain[29,52]

$$\hat{O}^{NR}(\hat{H}^{J}) = \hat{H}^{BO-J} = \hat{H}^{BO-L} + \hat{H}^{BO-S}, \quad (28)$$

with $\hat{H}^{BO-L}$ and $\hat{H}^{BO-S}$ being the Born–Oppenheimer perturbations due to the rotation of the nuclear system and are associated with the total electronic orbital (with respect to the molecular center of mass) and spin angular momenta.

The LRESC series expansion of $\boldsymbol{M}_N^{PV(e-e)}$ in terms of c^{-2} may then be obtained from

$$\boldsymbol{M}_N^{PV(e-e)} = -\hbar\frac{\partial^2}{\partial\boldsymbol{I}_N\partial\boldsymbol{J}}\left[\left\langle\left\langle\hat{O}^{NR}(\hat{H}^{PV})\,;\,\hat{O}^{NR}(\hat{H}^{J})\right\rangle\right\rangle\right] + \mathcal{O}(c^{-3}), \quad (29)$$

being the first term on the right-hand side of Eq. (29) the NR limit of $\boldsymbol{M}_N^{PV(e-e)}$. It will be named $\boldsymbol{M}_N^{PV-NR}$, and it is easy to see that it is the zeroth order contribution to $\boldsymbol{M}_N^{PV(e-e)}$ in a series expansion in terms of c^{-2},

$$\begin{aligned}\boldsymbol{M}_N^{PV-NR} &= -\hbar\frac{\partial^2}{\partial\boldsymbol{I}_N\partial\boldsymbol{J}}\left\langle\left\langle\hat{O}^{NR}(\hat{H}^{PV})\,;\,\hat{O}^{NR}(\hat{H}^{J})\right\rangle\right\rangle \\ &= -\hbar\frac{G_F\left(1-4\sin^2\theta_W\right)}{\sqrt{2}}\frac{1}{2mc}\lambda_N \\ &\quad\times\left(\left\langle\left\langle\{\boldsymbol{p}\,,\,\rho_N(\boldsymbol{r})\}\,;\,(\boldsymbol{r}-\boldsymbol{R}_{CM})\times\boldsymbol{p}\right\rangle\right\rangle\right. \\ &\quad\left.+\,\hbar^2\left\langle\left\langle\boldsymbol{\sigma}\times[\nabla\,,\,\rho_N(\boldsymbol{r})]\,;\,\frac{\boldsymbol{\sigma}}{2}\right\rangle\right\rangle\right)\cdot\boldsymbol{I}^{-1}. \end{aligned} \quad (30)$$

For closed-shell electronic structure molecules, only the first term on the right-hand side in the second line of Eq. (30) is nonzero. Then, for these kinds of systems, we have

$$\boldsymbol{M}_N^{PV-NR} = -\frac{G_F\left(1-4\sin^2\theta_W\right)}{\sqrt{2}}\frac{\hbar}{2mc}\lambda_N \times\left\langle\left\langle\{\boldsymbol{p}\,,\,\rho_N(\boldsymbol{r})\}\,;\,(\boldsymbol{r}-\boldsymbol{R}_{CM})\times\boldsymbol{p}\right\rangle\right\rangle_{\omega=0}\cdot\boldsymbol{I}^{-1}. \quad (31)$$

3. NR limit of the (p-p) contribution to M_N^{PV}

To derive the $(p-p)$ series expansion of a linear response function that involves the perturbed Hamiltonian $\hat{H}^{PV}$, this operator should be replaced into Eq. (19). Retaining only the zeroth order terms in the series expansion in terms of c^{-2}, the operator $\hat{X}(\hat{H}^{PV})$ will be proportional to

$$\hat{X}(\boldsymbol{\alpha}\cdot\boldsymbol{I}_N\,\rho_N(\boldsymbol{r})) = (2I+\beta)\,\boldsymbol{\alpha}\cdot\boldsymbol{I}_N\,\rho_N(\boldsymbol{r}), \quad (32)$$

with I and β being the 4×4 identity and Dirac matrices, respectively.

On the other hand, it is well-known that for $\hat{H}^{J}$ we have, retaining only the zeroth order expansion terms,[29] that

$$\hat{X}(\hat{H}^{J}) = -2\,\boldsymbol{\omega}\cdot\boldsymbol{J}_e. \quad (33)$$

From Eqs. (32) and (33), and taking into account that only $\hat{H}_{LS}$ and $\hat{X}_{SL}(\hat{H})$ are involved in Eq. (20), it can be shown that for the perturbation operators needed to derive the NR limit of the PV-NSR tensor [given in Eqs. (7) and (9)], we have

$$\hat{H}_{LS}^{PV} = -\frac{G_F\left(1-4\sin^2\theta_W\right)}{\sqrt{2}}\sum_N\lambda_N\,\boldsymbol{\sigma}\cdot\boldsymbol{I}_N\,\rho_N(\boldsymbol{r}), \quad (34)$$

$$\hat{H}_{LS}^{J} = 0, \quad (35)$$

$$\hat{X}_{SL}(\hat{H}^{PV}) = \boldsymbol{\sigma}\cdot\boldsymbol{I}_N\,\boldsymbol{\rho}_N(\boldsymbol{r}), \quad (36)$$

$$\hat{X}_{SL}(\hat{H}^{J}) = 0. \quad (37)$$

As it was stated below, the $(p-p)$ contributions to $\boldsymbol{M}_N^{PV}$ may be expanded in a series in terms of c^{-2} employing the LRESC model. This expansion will be obtained by replacing Eqs. (34)–(37) into Eq. (20). In this way, we get[51,52]

$$\left\langle\left\langle\,\hat{H}^{PV}\,;\,\hat{H}^{J}\,\right\rangle\right\rangle^{(p-p)} = 0 + \mathcal{O}(c^{-3}). \quad (38)$$

Finally, as

$$\begin{aligned}\boldsymbol{M}_N^{PV(p-p)} &\simeq -\hbar\frac{\partial^2}{\partial\boldsymbol{I}_N\partial\boldsymbol{J}}\left(\left\langle\left\langle\,\hat{H}^{PV}\,;\,\hat{H}^{J}\,\right\rangle\right\rangle^{(p-p)}\right) \\ &= 0+\mathcal{O}(c^{-3}),\end{aligned} \quad (39)$$

and as the NR limit of $\boldsymbol{M}_N^{PV}$ is of order c^{-1} [see Eq. (30)], then the result of Eq. (39) implies that the NR limit of $\boldsymbol{M}_N^{PV(p-p)}$ is exactly zero. The same behavior is observed for the parity-conserving NSR tensor, $\boldsymbol{M}_N^{(p-p)}$.[29]

An additional comment that should be emphasized is related to the comparison between the NR limits of the PV-NMR-shielding and PV-NSR tensors. It can be shown that for molecules with closed-shell electronic structures, the NR limit of Eq. (13) is given by

$$\boldsymbol{\sigma}_N^{PV-NR-para} = -\frac{G_F\left(1-4\sin^2\theta_W\right)}{\sqrt{2}}\frac{m_p}{2\,\hbar\,m^2\,c}\frac{1}{g_N}\lambda_N \times\left\langle\left\langle\{\boldsymbol{p}\,,\,\rho_N(\boldsymbol{r})\}\,;\,(\boldsymbol{r}-\boldsymbol{R}_{GO})\times\boldsymbol{p}\right\rangle\right\rangle_{\omega=0}. \quad (40)$$

It is evident that the PV-NMR-shielding and PV-NSR tensors are closely related to each other in the NR limit when the gauge origin of the magnetic potential is placed at the molecular CM.[19] It happens exactly as in the case of the parity-conserving analogous properties, $\boldsymbol{\sigma}_N^{NR-para}$ and $\boldsymbol{M}_N^{NR-elec}$, which are related by the well-known Ramsey–Flygare relationship.[29,55,56] Actually, the NR relation between $\boldsymbol{\sigma}_N^{PV-NR-para}$ and $\boldsymbol{M}_N^{PV-NR}$ is given by

$$\boldsymbol{\sigma}_N^{PV-NR-para} = \frac{m_p}{m\hbar^2}\frac{1}{g_N}\boldsymbol{M}_N^{PV-NR}\cdot\boldsymbol{I}. \quad (41)$$

As it can be seen in the NR expressions of the PV-NMR-shielding [Eq. (40)] and PV-NSR tensors [Eq. (31)],

the only difference between their linear response functions appears in the electronic orbital angular momentum operator. For the PV-NSR tensor, this operator may be evaluated with respect to the molecular CM and not with respect to the gauge origin, as it was reported in previous works.[16,19]

III. COMPUTATIONAL DETAILS

The H_2X_2 series of molecules (with X = ^{17}O, ^{33}S, ^{77}Se, ^{125}Te, and ^{209}Po) was studied at different dihedral angles, with fixed bond lengths and H–X–X angles taken from Ref. 35 and given in Table I. The dihedral angles α of the C_2 symmetric P-conformations are taken in steps of 15° while keeping constant all the remaining internal structural parameters.

The employed nuclear g-factors were taken from Ref. 57. Their values are −0.757 516 for ^{17}O, 0.429 214 for ^{33}S, 1.070 084 for ^{77}Se, −1.7771 for ^{125}Te, and 1.376 for ^{209}Po.

All the calculations of $\boldsymbol{\sigma}^{PV}$ and $\boldsymbol{M}^{PV}$ have been performed using a development version of the DIRAC program package.[58,59] In all calculations, we have employed Dyall's relativistic aae2z, aae3z, and aae4z uncontracted basis sets (dyall.aae2z, dyall.aae3z, and dyall.aae4z) for hydrogen (unpublished), oxygen, sulfur,[60] selenium, tellurium, and polonium.[61–64] The common gauge origin approach was used, and the gauge origin for the external magnetic potential has always been placed at the center of the nucleus of interest.

The Dirac–Coulomb (DC), spin-free (SF), and Lévy–Leblond (LL) Hamiltonians have been employed;[65] we used the former two in order to disentangle the SF and the SO effects on the calculated constants. In the DC and SF calculations, the (SS|SS) integrals were eliminated in both the self-consistent field and the linear response parts. It is the default choice in the DIRAC code, and an energy correction is used to avoid the explicit calculation of these integrals.[66]

The small component basis sets for the relativistic calculations were generated by applying separately unrestricted kinetic balance (UKB)[54] and restricted kinetic balance (RKB) prescriptions. The SF calculations were performed using RKB. The Gaussian nuclear (GN) charge distribution model was used to obtain all the results in this work,[67] but in order to compare with previous results, the point-charge nuclear (PN) model was also employed in the NR calculations.

The response calculations were carried out at the 4c polarization propagator RPA level of theory employing the Dirac–Hartree–Fock wave functions. NR values of $\boldsymbol{\sigma}^{PV}$ and $\boldsymbol{M}^{PV}$ tensor elements were obtained employing the LL Hamiltonian.

For studying the influence of electron correlation effects, Dirac–Kohn–Sham-DFT calculations were performed based on the 4c-DC, 4c-SF, and NR-LL Hamiltonians. We used two NR exchange–correlation functionals: the generalized-gradient-approximation functional KT3[68] and the hybrid functional PBE0.[69]

TABLE I. Structural parameters for the H_2X_2 molecules (X = ^{17}O, ^{33}S, ^{77}Se, ^{125}Te, and ^{209}Po) used in the calculations of the PV-NSR and PV-NMR-shielding constants.

	H_2O_2	H_2S_2	H_2Se_2	H_2Te_2	H_2Po_2
X–H (Å)	0.97	1.352	1.45	1.64	1.74
X–X (Å)	1.49	2.055	2.48	2.84	2.91
θ(HXX) (deg)	100	92	92	92	92

These functionals were selected due to their good performance in the 4c calculations of parity-conserving NSR constants, compared with experimental values.[70,71]

The response of Eq. (4) was solved with respect to the property gradient associated with the total electronic orbital and spin angular momenta (to calculate $\boldsymbol{M}_N^{PV}$) and with the external magnetic field (for $\boldsymbol{\sigma}_N^{PV}$).

IV. RESULTS AND DISCUSSION

To the best of our knowledge, this work reports for the first time the relativistic theory and calculations of the PV-NSR constants. We have chosen the set of nuclei X = ^{17}O, ^{33}S, ^{77}Se, ^{125}Te, and ^{209}Po in the H_2X_2 molecules to test our PV-NSR implementation and to investigate the behavior of these properties. Alongside the PV-NSR calculations, we also calculated the PV contributions to the NMR (isotropic) shieldings in the same set of molecules, as similar calculations have been presented in a number of previous works.[23,25–27]

TABLE II. PV-NSR (isotropic) constants [M_{iso}^{PV}(Se), in μHz] for the ^{77}Se nucleus in the P enantiomer of H_2Se_2 for a dihedral angle of 45°. The DC Hamiltonian was used.

	RPA		PBE0		KT3	
Basis set	RKB	UKB	RKB	UKB	RKB	UKB
cc-pVDZ	−1.97	−1.97	1.05	1.05	2.36	2.36
aug-cc-pVDZ	−1.04	−1.04	1.42	1.42	2.59	2.59
cc-pVTZ	−2.03	−2.03	0.86	0.86	2.41	2.41
aug-cc-pVTZ	−1.94	−1.94	0.78	0.78	2.18	2.18
cc-pVQZ	−2.03	−2.03	0.86	0.86	2.35	2.35
aug-cc-pVQZ	−2.04	−2.04[a]	0.79	0.79	2.24	2.24
cc-pV5Z	−2.10	−2.10	0.83	0.83	2.35	2.35
aug-cc-pV5Z	−2.13	−2.13	0.78	0.78	2.27	2.27
dyall.v2z	−1.91	−1.91	1.36	1.36	2.92	2.92
dyall.cv2z	−2.14	−2.14	1.08	1.08	2.68	2.68
dyall.av2z	−1.09	−1.09	1.56	1.56	2.93	2.93
dyall.acv2z	−1.33	−1.33	1.29	1.29	2.70	2.70
dyall.ae2z	−2.14	−2.14	1.08	1.08	2.68	2.68
dyall.aae2z	−1.33	−1.33	1.29	1.29	2.70	2.70
dyall.v3z	−2.19	−2.19	1.01	1.01	2.72	2.72
dyall.cv3z	−2.38	−2.38	0.82	0.82	2.54	2.54
dyall.av3z	−2.16	−2.16	0.89	0.89	2.48	2.48
dyall.acv3z	−2.35	−2.35	0.71	0.71	2.30	2.30
dyall.ae3z	−2.38	−2.38	0.82	0.82	2.54	2.54
dyall.aae3z	−2.35	−2.35	0.71	0.71	2.30	2.30
dyall.v4z	−2.29	−2.29	0.92	0.92	2.59	2.59
dyall.cv4z	−2.48	−2.48	0.74	0.74	2.39	2.39
dyall.av4z	−2.29	−2.29[a]	0.90	0.90	2.55	2.55
dyall.acv4z	−2.48	−2.47	0.72	0.72	2.36	2.36
dyall.ae4z	−2.48	−2.48	0.74	0.74	2.40	2.40
dyall.aae4z	−2.48	−2.48	0.72	0.72	2.36	2.36

[a]Calculations with quasi-instabilities.

In order to test the basis set convergence of $M_{iso}^{PV}(X)$, we looked at the special case of $X = {}^{77}$Se in the H_2Se_2 molecule at a dihedral angle of 45°. We have performed calculations employing the DC Hamiltonian at the RPA, DFT-PBE0, and DFT-KT3 levels of theory using a finite Gaussian nuclear model. These results are given in Table II for the various quality uncontracted basis sets, used for both ^{1}H and ^{77}Se atoms: dyall.vYz (valence), dyall.cv$Y$z (core-valence), dyall.av$Y$z (valence with extra diffuse functions), dyall.acv$Y$z (core-valence with additional diffuse functions), dyall.ae$Y$z (all-electron, meaning that they include correlating functions for all shells), and dyall.aae$Y$z (all-electron with extra diffuse functions), with Y = 2, 3, and 4 referring to double-zeta, triple-zeta, and quadruple-zeta qualities, respectively.[60] For the sake of comparison with previous works, some correlation-consistent polarized Dunning's (valence-only) basis sets were also used: cc-pVWZ and aug-cc-pVWZ (W = D, T, Q, and 5).[72,73] Instabilities of the Kramer's restricted DHF wave functions appear in some of the RPA calculations. They can be avoided by manually modifying some of the exponents of the basis sets or by performing calculations applying the pure zeroth order approach (PZOA), but this is out of the scope of the present work. Nevertheless, in those cases where quasi-instabilities appear for RPA calculations, reliable DFT values allow the analysis of the complete sets of results even for large basis sets.

For Dyall's basis sets, we observe good convergence with the principle number, with the difference between the v4z and the v3z basis sets just 0.09–0.13 μHz, depending on the method. Addition of diffuse functions has an effect of about 10% on the v3z quality basis set (when using PBE0-KT3) but becomes negligible in relation to the v4z basis. Finally, while adding correlation functions for the core-valence region lowers the results significantly (cv$Y$z vs vYz basis), further increase in the number of correlating functions (ae$Y$z vs cv$Y$z basis) has a negligible effect. This leads us to conclude that in cases where computational costs are an important factor the choice of either dyall.acv3z or dyall.cv4z is justified. Here, as we are dealing with small systems, we proceed with the ae$Y$z basis sets.

The choice of functional has a significant effect on the absolute values of the PV isotropic NSR constants at a given geometry; later on, we will observe that the trends and behavior are consistent across the method used in this work.

Tables III and IV show $\sigma_{iso}^{PV}(X)$ and $M_{iso}^{PV}(X)$ for all the molecules studied in this work, at a dihedral angle of 45°. We present results obtained using the DC, SF, and LL Hamiltonians at the RPA and DFT-PBE0 levels of theory. The latter provide a comparison between the *ab initio* (RPA) and the DFT calculations. DFT-PBE0 was chosen instead of DFT-KT3 because while both reproduce experimental parity-conserving NSR constants in a good fashion, DFT-PBE0 calculations show a better performance.[70,71] In all these calculations, the finite Gaussian nuclear model was employed. The basis set convergence of $\sigma_{iso}^{PV}(X)$ and

TABLE III. PV isotropic shielding constants ($\sigma_{iso}^{PV}(X)$, in ppm) for the X nuclei in the P enantiomers of H_2X_2 molecules ($X = {}^{17}$O, ^{33}S, ^{77}Se, ^{125}Te, and ^{209}Po) for a dihedral angle of 45°. The dyall.aae$Y$z (Y = 2, 3, and 4) basis sets were employed.

		RPA				PBE0			
Mol.	Basis	DC (UKB)	DC (RKB)	SF (RKB)	NR (GN)	DC (UKB)	DC (RKB)	SF (RKB)	NR (GN)
H_2O_2	aae2z	5.06×10^{-9}	5.07×10^{-9}	5.27×10^{-9}	5.21×10^{-9}	4.95×10^{-9}	4.96×10^{-9}	5.46×10^{-9}	5.40×10^{-9}
	aae3z	5.39×10^{-9}	5.40×10^{-9}	5.58×10^{-9}	5.51×10^{-9}	5.25×10^{-9}	5.26×10^{-9}	5.79×10^{-9}	5.72×10^{-9}
	aae4z	5.64×10^{-9}	5.64×10^{-9}	5.83×10^{-9}	5.75×10^{-9}	5.50×10^{-9}	5.50×10^{-9}	6.06×10^{-9}	5.97×10^{-9}
	Bast *et al.*[a]	6.06×10^{-9}	6.06×10^{-9}	6.23×10^{-9}	6.12×10^{-9}[b]				
H_2S_2	aae2z	-7.98×10^{-8}	-7.98×10^{-8}	-8.63×10^{-8}	-8.26×10^{-8}	-8.03×10^{-8}	-8.03×10^{-8}	-8.74×10^{-8}	-8.37×10^{-8}
	aae3z	-9.00×10^{-8}	-9.01×10^{-8}	-9.67×10^{-8}	-9.13×10^{-8}	-9.01×10^{-8}	-9.01×10^{-8}	-9.74×10^{-8}	-9.19×10^{-8}
	aae4z	-9.47×10^{-8}	-9.47×10^{-8}	-1.01×10^{-7}	-9.49×10^{-8}	-9.47×10^{-8}	-9.47×10^{-8}	-1.02×10^{-7}	-9.54×10^{-8}
	Bast *et al.*[a]	-9.98×10^{-8}	-9.98×10^{-8}	-1.05×10^{-7}	-9.75×10^{-8}[b]				
H_2Se_2	aae2z	3.13×10^{-8}	3.13×10^{-8}	-2.37×10^{-7}	-1.87×10^{-7}	7.31×10^{-9}	7.31×10^{-9}	-2.61×10^{-7}	-2.05×10^{-7}
	aae3z	1.19×10^{-8}	1.19×10^{-8}	-2.61×10^{-7}	-1.97×10^{-7}	-1.05×10^{-8}	-1.05×10^{-8}	-2.82×10^{-7}	-2.12×10^{-7}
	aae4z	1.17×10^{-8}	1.17×10^{-8}	-2.68×10^{-7}	-1.99×10^{-7}	-1.21×10^{-8}	-1.21×10^{-8}	-2.89×10^{-7}	-2.14×10^{-7}
	Bast *et al.*[a]	1.25×10^{-8}	1.25×10^{-8}	-2.72×10^{-7}	-2.00×10^{-7}[b]				
H_2Te_2	aae2z	-9.60×10^{-7}	-9.60×10^{-7}	5.75×10^{-7}	3.08×10^{-7}	-1.22×10^{-6}	-1.22×10^{-6}	6.30×10^{-7}	3.38×10^{-7}
	aae3z	-1.24×10^{-6}	-1.25×10^{-6}	6.04×10^{-7}	3.12×10^{-7}	-9.38×10^{-7}	-9.38×10^{-7}	6.49×10^{-7}	3.34×10^{-7}
	aae4z	-1.26×10^{-6}	-1.26×10^{-6}	6.11×10^{-7}	3.12×10^{-7}	-9.50×10^{-7}	-9.50×10^{-7}	6.55×10^{-7}	3.33×10^{-7}
	Bast *et al.*[a]	-1.29×10^{-6}	-1.29×10^{-6}	6.13×10^{-7}	3.15×10^{-7}[b]				
H_2Po_2	aae2z	8.34×10^{-4}	8.34×10^{-4}	-5.95×10^{-6}	-1.11×10^{-6}	6.85×10^{-5}	6.85×10^{-5}	-6.44×10^{-6}	-1.20×10^{-6}
	aae3z	1.66×10^{-3}	1.66×10^{-3}	-5.93×10^{-6}	-1.12×10^{-6}	6.63×10^{-5}	6.63×10^{-5}	-6.30×10^{-6}	-1.18×10^{-6}
	aae4z	1.54×10^{-3}	1.54×10^{-3}	-5.91×10^{-6}	-1.12×10^{-6}	6.57×10^{-5}	6.57×10^{-5}	-6.28×10^{-6}	-1.18×10^{-6}
	Bast *et al.*[a]	1.28×10^{-3}	1.25×10^{-3}	-5.25×10^{-6}	-9.95×10^{-7}[b]				

[a]Taken from the most converged results at Table I of Ref. 26.
[b]Calculated using PN instead of GN (see Ref. 26).

TABLE IV. PV-NSR (isotropic) constants [$M_{iso}^{PV}(X)$, in Hz] for the X nuclei in the P enantiomers of H_2X_2 molecules (X = ^{17}O, ^{33}S, ^{77}Se, ^{125}Te, and ^{209}Po) for a dihedral angle of 45°. The dyall.aae$Y$z (Y = 2, 3, and 4) basis sets were employed.

		RPA				PBE0			
Mol.	Basis	DC (UKB)	DC (RKB)	SF (RKB)	NR (GN)	DC (UKB)	DC (RKB)	SF (RKB)	NR (GN)
H_2O_2	aae2z	-4.18×10^{-7}	-4.18×10^{-7}	-4.50×10^{-7}	-4.53×10^{-7}	-3.27×10^{-7}	-3.27×10^{-7}	-3.65×10^{-7}	-3.70×10^{-7}
	aae3z	-4.60×10^{-7}	-4.60×10^{-7}	-4.94×10^{-7}	-4.95×10^{-7}	-3.65×10^{-7}	-3.65×10^{-7}	-4.04×10^{-7}	-4.09×10^{-7}
	aae4z	-4.82×10^{-7}	-4.82×10^{-7}	-5.18×10^{-7}	-5.18×10^{-7}	-3.82×10^{-7}	-3.82×10^{-7}	-4.24×10^{-7}	-4.27×10^{-7}
H_2S_2	aae2z	-2.39×10^{-6}	-2.39×10^{-6}	-2.50×10^{-6}	-2.42×10^{-6}	-2.50×10^{-6}	-2.50×10^{-6}	-2.62×10^{-6}	-2.56×10^{-6}
	aae3z	-2.61×10^{-6}	-2.61×10^{-6}	-2.71×10^{-6}	-2.59×10^{-6}	-2.74×10^{-6}	-2.74×10^{-6}	-2.86×10^{-6}	-2.75×10^{-6}
	aae4z	-2.74×10^{-6}	-2.74×10^{-6}	-2.84×10^{-6}	-2.69×10^{-6}	-2.88×10^{-6}	-2.88×10^{-6}	-2.99×10^{-6}	-2.85×10^{-6}
H_2Se_2	aae2z	-1.33×10^{-6}	-1.33×10^{-6}	-9.53×10^{-6}	-8.28×10^{-6}	1.29×10^{-6}	1.29×10^{-6}	-8.65×10^{-6}	-7.93×10^{-6}
	aae3z	-2.35×10^{-6}	-2.35×10^{-6}	-1.03×10^{-5}	-8.54×10^{-6}	7.12×10^{-7}	7.12×10^{-7}	-9.40×10^{-6}	-8.19×10^{-6}
	aae4z	-2.48×10^{-6}	-2.48×10^{-6}	-1.06×10^{-5}	-8.60×10^{-6}	7.24×10^{-7}	7.24×10^{-7}	-9.63×10^{-6}	-8.25×10^{-6}
H_2Te_2	aae2z	4.27×10^{-5}	4.27×10^{-5}	-2.87×10^{-5}	-1.89×10^{-5}	2.47×10^{-5}	2.47×10^{-5}	-2.65×10^{-5}	-1.95×10^{-5}
	aae3z	2.15×10^{-5}	2.15×10^{-5}	-2.95×10^{-5}	-1.85×10^{-5}	4.15×10^{-5}	4.15×10^{-5}	-2.73×10^{-5}	-1.91×10^{-5}
	aae4z	2.18×10^{-5}	2.18×10^{-5}	-2.96×10^{-5}	-1.84×10^{-5}	4.21×10^{-5}	4.21×10^{-5}	-2.74×10^{-5}	-1.90×10^{-5}
H_2Po_2	aae2z	2.27×10^{-3}	2.27×10^{-3}	-1.17×10^{-4}	-4.81×10^{-5}	1.85×10^{-3}	1.85×10^{-3}	-7.28×10^{-5}	-4.99×10^{-5}
	aae3z	2.67×10^{-3}[a]	2.67×10^{-3}[a]	-1.15×10^{-4}	-4.64×10^{-5}	1.79×10^{-3}	1.79×10^{-3}	-7.30×10^{-5}	-4.82×10^{-5}
	aae4z	2.59×10^{-3}[a]	2.59×10^{-3}[a]	-1.14×10^{-4}	-4.60×10^{-5}	1.77×10^{-3}	1.77×10^{-3}	-7.22×10^{-5}	-4.79×10^{-5}

[a]Calculations with quasi-instabilities.

$M_{iso}^{PV}(X)$ is studied for the dyall.aae$Y$z (Y = 2, 3, and 4) basis sets. We also compare our results with the previous work of Bast and colleagues.[26]

Two values, employing RKB and UKB prescriptions, are given for each DC calculation. Using the RKB prescription, the small component basis set is obtained from the NR limit of the coupling between large and small components of the wave function. It is known that when an external vector potential is introduced in the Dirac equation, the RKB prescription may lead to non-converged NMR shieldings,[54,74] and in those cases, the UKB calculations ensure a better coupling of small and large components. It is also known that the differences between RKB and UKB calculations decrease as the basis set quality increases.[75] In Tables III and IV, it is observed that results employing the DC Hamiltonian with RKB and UKB prescriptions have differences smaller than 1% for $\sigma_{iso}^{PV}(X)$ in all combinations of molecules and basis sets for both RPA and PBE0 levels of theory. These differences are even smaller in $M_{iso}^{PV}(X)$ than in $\sigma_{iso}^{PV}(X)$.

Our results are in good agreement with those of Bast, Schwerdtfeger, and Saue for the PV NMR shieldings.[26] The small differences

TABLE V. PV-NSR (isotropic) constants [$M_{iso}^{PV}(X)$, in Hz] for the ^{33}S and ^{77}Se nuclei in the P enantiomers of H_2S_2 and H_2Se_2 molecules for various dihedral angles α. The results were obtained using the dyall.aae4z basis set.

	H_2S_2				H_2Se_2			
	RPA		PBE0		RPA		PBE0	
α (deg)	DC (UKB)	NR (GN)	DC (UKB)	NR (GN)	DC (UKB)	NR (GN)	DC (UKB)	NR (GN)
15	-1.14×10^{-6}	-1.14×10^{-6}	-1.21×10^{-6}	-1.21×10^{-6}	6.57×10^{-7}	-3.56×10^{-6}	2.12×10^{-6}	-3.47×10^{-6}
30	-2.08×10^{-6}	-2.07×10^{-6}	-2.20×10^{-6}	-2.20×10^{-6}	-5.58×10^{-8}	-6.54×10^{-6}	2.52×10^{-6}	-6.33×10^{-6}
45	-2.74×10^{-6}	-2.69×10^{-6}	-2.88×10^{-6}	-2.85×10^{-6}	-2.48×10^{-6}	-8.60×10^{-6}	7.24×10^{-7}	-8.25×10^{-6}
60	-3.11×10^{-6}	-3.01×10^{-6}	-3.25×10^{-6}	-3.18×10^{-6}	-6.14×10^{-6}	-9.71×10^{-6}	-2.70×10^{-6}	-9.20×10^{-6}
75	-3.23×10^{-6}	-3.08×10^{-6}	-3.37×10^{-6}	-3.24×10^{-6}	-1.04×10^{-5}	-1.00×10^{-5}	-6.93×10^{-6}	-9.37×10^{-6}
90	-3.18×10^{-6}	-2.97×10^{-6}	-3.31×10^{-6}	-3.12×10^{-6}	-1.47×10^{-5}	-9.76×10^{-6}	-1.13×10^{-5}	-8.96×10^{-6}
105	-2.99×10^{-6}	-2.73×10^{-6}	-3.10×10^{-6}	-2.86×10^{-6}	-1.86×10^{-5}	-9.03×10^{-6}	-1.52×10^{-5}	-8.13×10^{-6}
120	-2.67×10^{-6}	-2.37×10^{-6}	-2.77×10^{-6}	-2.49×10^{-6}	-2.12×10^{-5}	-7.91×10^{-6}	-1.79×10^{-5}	-6.98×10^{-6}
135	-2.22×10^{-6}	-1.92×10^{-6}	-2.30×10^{-6}	-2.01×10^{-6}	-2.16×10^{-5}	-6.42×10^{-6}	-1.85×10^{-5}	-5.55×10^{-6}
150	-1.61×10^{-6}	-1.36×10^{-6}	-1.68×10^{-6}	-1.43×10^{-6}	-1.84×10^{-5}	-4.55×10^{-6}	-1.58×10^{-5}	-3.87×10^{-6}
165	-8.56×10^{-7}	-7.10×10^{-7}	-8.91×10^{-7}	-7.50×10^{-7}	-1.08×10^{-5}	-2.37×10^{-6}	-9.30×10^{-6}	-1.99×10^{-6}

TABLE VI. Same as in Table V but for ^{125}Te and ^{209}Po nuclei in H_2Te_2 and H_2Po_2 molecules.

	H_2Te_2				H_2Po_2			
	RPA		PBE0		RPA		PBE0	
α (deg)	DC (UKB)	NR (GN)	DC (UKB)	NR (GN)	DC (UKB)	NR (GN)	DC (UKB)	NR (GN)
15	2.15×10^{-5}	-7.68×10^{-6}	3.15×10^{-5}	-8.08×10^{-6}	7.27×10^{-4}[a]	-1.97×10^{-5}	1.21×10^{-3}	-2.08×10^{-5}
30	2.98×10^{-5}	-1.40×10^{-5}	4.69×10^{-5}	-1.47×10^{-5}	9.62×10^{-4}[a]	-3.55×10^{-5}	1.81×10^{-3}	-3.73×10^{-5}
45	2.18×10^{-5}	-1.84×10^{-5}	4.21×10^{-5}	-1.90×10^{-5}	2.59×10^{-3}[a]	-4.60×10^{-5}	1.77×10^{-3}	-4.79×10^{-5}
60	1.29×10^{-6}	-2.07×10^{-5}	2.22×10^{-5}	-2.12×10^{-5}	1.51×10^{-3}[a]	-5.16×10^{-5}	1.34×10^{-3}	-5.32×10^{-5}
75	-2.63×10^{-5}	-2.15×10^{-5}	-6.11×10^{-6}	-2.18×10^{-5}	7.70×10^{-4}	-5.36×10^{-5}	7.18×10^{-4}	-5.46×10^{-5}
90	-5.69×10^{-5}	-2.12×10^{-5}	-3.75×10^{-5}	-2.11×10^{-5}	-3.96×10^{-5}	-5.30×10^{-5}	2.26×10^{-5}	-5.34×10^{-5}
105	-8.67×10^{-5}	-1.99×10^{-5}	-6.76×10^{-5}	-1.96×10^{-5}	-8.61×10^{-4}	-5.04×10^{-5}	-6.76×10^{-4}	-5.02×10^{-5}
120	-1.11×10^{-4}	-1.78×10^{-5}	-9.16×10^{-5}	-1.72×10^{-5}	-1.59×10^{-3}[a]	-4.56×10^{-5}	-1.30×10^{-3}	-4.50×10^{-5}
135	-1.21×10^{-4}	-1.47×10^{-5}	-1.03×10^{-4}	-1.41×10^{-5}	-2.22×10^{-3}[a]	-3.84×10^{-5}	-1.72×10^{-3}	-3.75×10^{-5}
150	-1.08×10^{-4}	-1.06×10^{-5}	-9.27×10^{-5}	-1.01×10^{-5}	-2.14×10^{-3}[a]	-2.83×10^{-5}	-1.74×10^{-3}	-2.74×10^{-5}
165	-6.53×10^{-5}	-5.60×10^{-6}	-5.63×10^{-5}	-5.27×10^{-6}	-1.38×10^{-3}[a]	-1.51×10^{-5}	-1.14×10^{-3}	-1.46×10^{-5}

[a]Calculations with quasi-instabilities.

are due to their use of contracted Dunning's basis sets, whereas we used uncontracted basis sets.

For the lighter molecules, relativistic effects play a small role only, and the DC, SF, and NR results are generally in good agreement. However, their influence becomes more significant from H_2Se_2, with the SO interaction dominating for both properties.

For the NR results, we have furthermore analyzed the differences between modeling the electric charge distribution of the nuclei as points or using Gaussian spherically symmetric functions. These models are used for both the electron–nucleus Coulomb interaction and the electric nuclear density distribution $\rho_N(\boldsymbol{r})$ given in the linear response functions of Eqs. (10) and (13). The differences in the results obtained for the two nuclear models are less than 0.004% for O, 0.05% for S, 0.22% for Se, 0.53% for Te, and 1.1% for Po, for both σ_{iso}^{PV-NR} and M_{iso}^{PV-NR} (see Tables I–X of the supplementary material).

In Tables V and VI, we show calculations of $M_{iso}^{PV}(X)$ and $M_{iso}^{PV-NR}(X)$ for the nuclei X = ^{33}S, ^{77}Se, ^{125}Te, and ^{209}Po in the H_2X_2 series of molecules at different dihedral angles between 0° and 180°. Because of mirror symmetry of these systems, the PV contributions to the isotropic NSR constants is bound to be zero for dihedral angles α of 0° and 180°. All the results given in Tables V and VI were obtained using the biggest basis set employed in this work, the dyall.aae4z one. The RPA and DFT-PBE0 calculations are shown in order to compare electron correlation effects.

A comparison between equivalent calculations of M_{iso}^{PV} and σ_{iso}^{PV} for different dihedral angles is given in Figs. 1–3 for Se, Te, and Po,

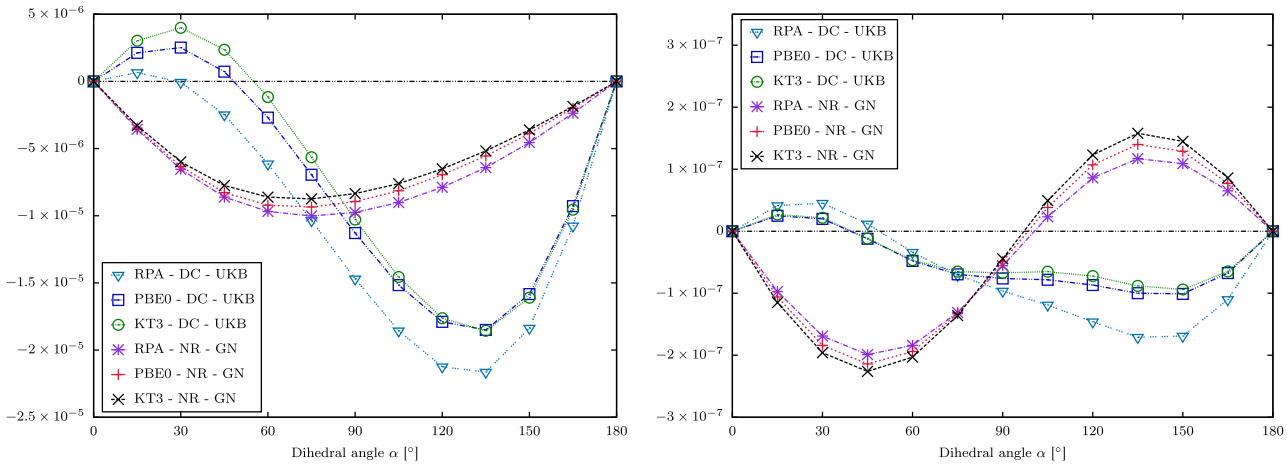

FIG. 1. (a) M_{iso}^{PV} (in Hz) and (b) σ_{iso}^{PV} (in ppm) for selenium-77 in H_2Se_2 at different dihedral angles employing the DC and LL Hamiltonians at the RPA, DFT-PBE0, and DFT-KT3 levels of approach and using the dyall.aae4z basis set.

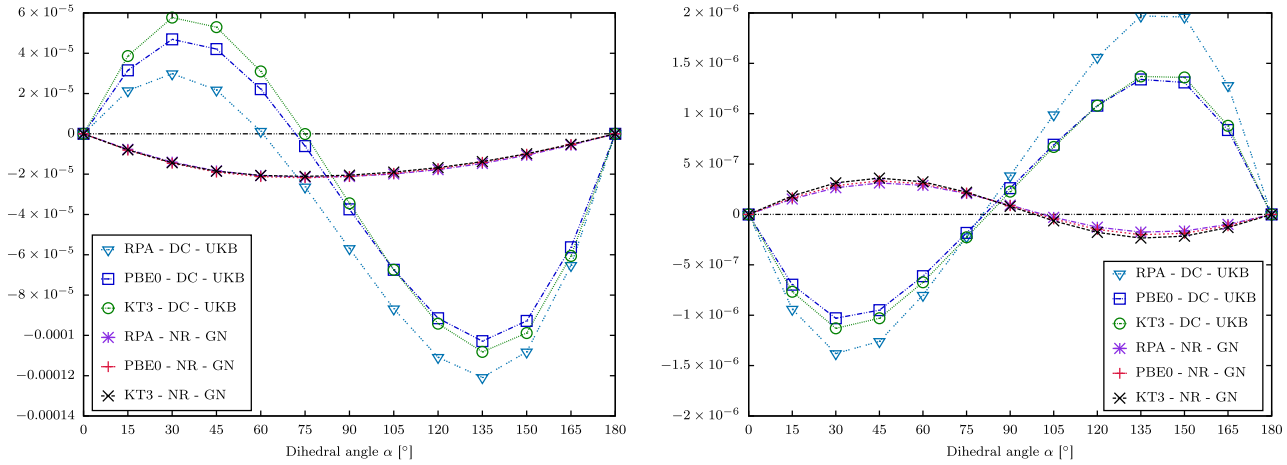

FIG. 2. Same as in Fig. 1, but for (a) M_{iso}^{PV} (in Hz) and (b) σ_{iso}^{PV} (in ppm) for tellurium-125 in H_2Te_2.

respectively. In Figs. 1–3, we compare the (4c-) Dirac–Coulomb and (NR-) Lévy–Leblond calculations at the RPA (only for Se and Te), DFT-PBE0, and DFT-KT3 levels of theory. There is a major difference between the NR limits of the PV contributions to NSR and NMR shieldings: The NR limits of M_{iso}^{PV} have a dependence with the dihedral angle α that behaves as a function $-\sin(\alpha)$, whereas for the NR limit of σ_{iso}^{PV} we observe a $-\sin(2\alpha)$-like dihedral angle dependence for Se and Po, while for tellurium this dependence behaves as $\sin(2\alpha)$.

The 4c calculations of the PV effects also show a different dependence on the dihedral angle for the two properties. It is important to stress at this point that whereas the PV-NMR-shielding constants are simply given by a linear response function [see Eq. (13)], the PV-NSR constants are obtained by multiplying a linear response function by the inverse of the inertia tensor $\boldsymbol{I}$ [see Eq. (10)]. As $\boldsymbol{I}$ changes with the dihedral angle α, the dependence of M_{iso}^{PV} on this angle is related to how both the linear response function of Eq. (10) and the inertia tensor change with it. One point to stress regarding Fig. 1(b) is that the non-smooth behavior found for the 4c-DFT calculations is due to partial cancellations of the SO and SF contributions, where the first is a function close to $\sin(2\alpha)$, whereas the SF contribution behaves as $-\sin(2\alpha)$, but with different maximum values, and also different roots.

The choice of correlation method (DFT-KT3 or DFT-PBE0) does not visibly affect the overall trend in these properties with

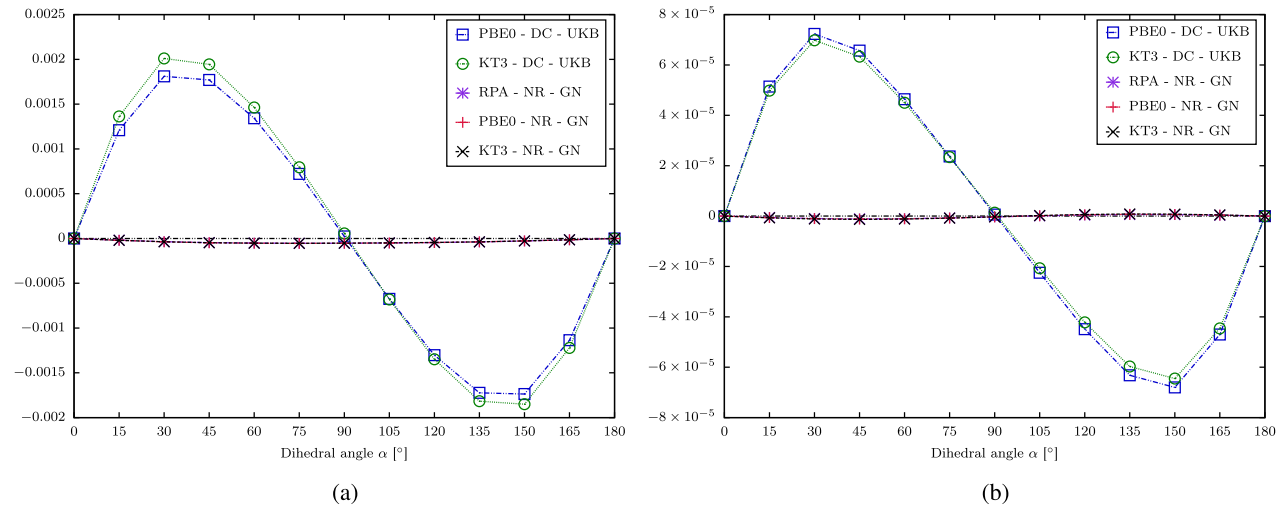

FIG. 3. Same as in Figs. 1 and 2, but for (a) M_{iso}^{PV} (in Hz) and (b) σ_{iso}^{PV} (in ppm) for polonium-209 in H_2Po_2.

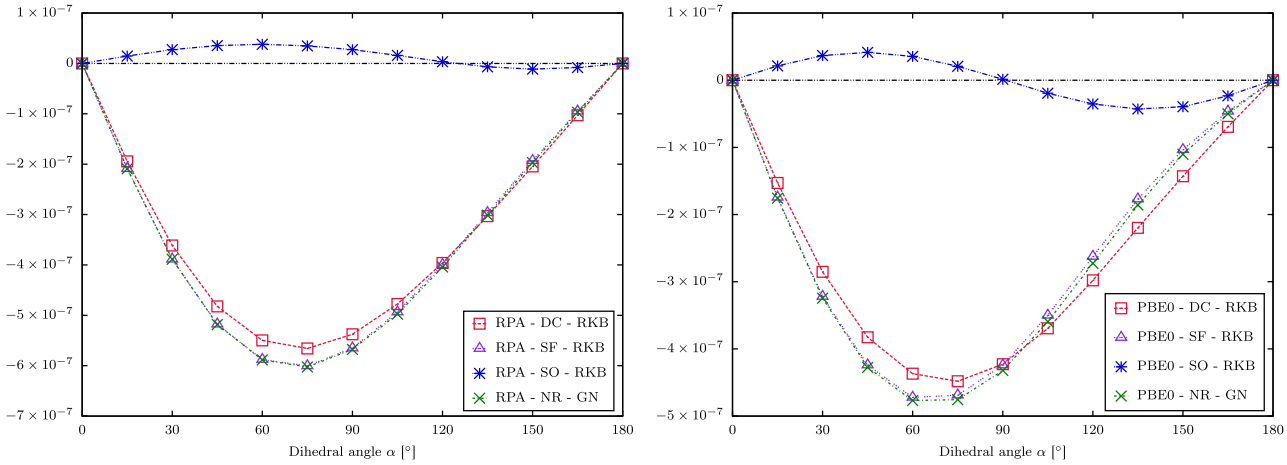

FIG. 4. Values of M_{iso}^{PV} (^{17}O) for H_2O_2 (in Hz) at different dihedral angles employing the DC, SF, and LL Hamiltonians at the (a) RPA and (b) DFT-PBE0 levels of approach, employing the dyall.aae4z basis set. The SO contribution is given as the difference between DC and SF calculations.

respect to the dihedral angle. Furthermore, even the effect of correlation altogether (difference between the RPA and the DFT results) is minor, except for H_2Se_2, where the x-intercept is shifted to higher angles for DFT.

In order to analyze relativistic effects on M_{iso}^{PV}, we compare the DC, SF, and NR calculations for all the molecules under study in this work. Their dependence on the dihedral angle is shown in Figs. 4–8. For oxygen, sulfur, selenium, and tellurium, we display both RPA and DFT-PBE0 calculations to investigate the electron correlation effects. For polonium, this was not possible because for the RPA calculations we found quasi-instabilities of Kramer's restricted DHF wave functions with respect to the time reversal odd perturbations, as was also reported in the past by Nahrwold and Berger.[27]

Even for the lightest nucleus, the oxygen, it can be seen in Fig. 4 that relativistic effects are not entirely negligible. If the DC results are split into the sum of SF and SO contributions, it can be seen that for the RPA and DFT-PBE0 calculations, almost all the relativistic effects of M_{iso}^{PV} (^{17}O) are due to the SO contribution, i.e., calculations employing the SF and LL Hamiltonians are almost the same.

In the case of sulfur, it is easily seen in Fig. 5 that the SF and SO contributions have similar maximum values. Nevertheless, the SF relativistic effects are always negative, whereas the SO effects behave as a $\sin(2\alpha)$ function, with a node at α between 75° and 90°.

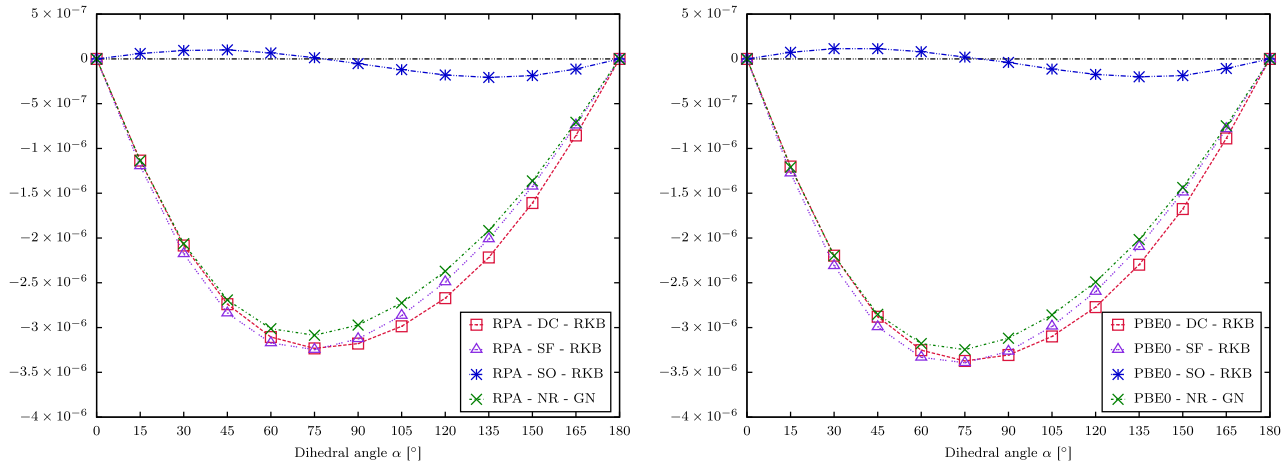

FIG. 5. Same as in Fig. 4, but for ^{33}S in H_2S_2 at the (a) RPA and (b) DFT-PBE0 levels of approach.

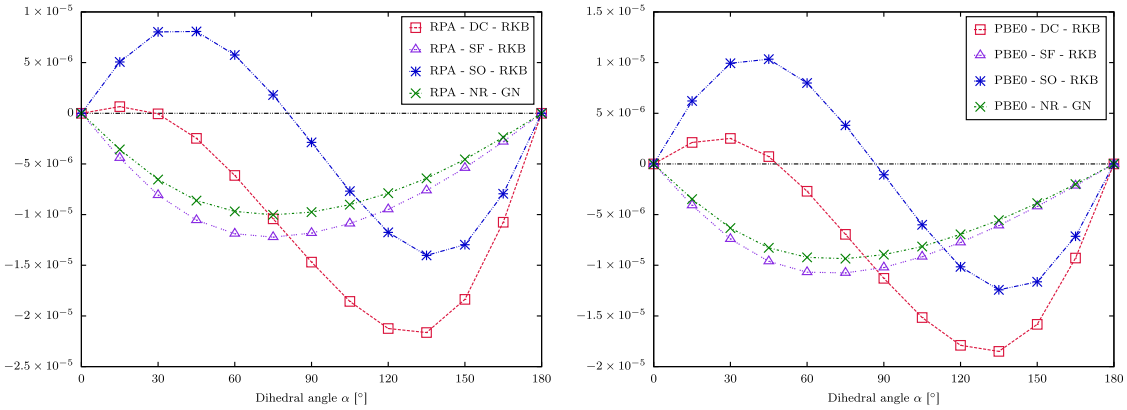

FIG. 6. Same as in Fig. 4, but for ^{77}Se in H_2Se_2 at the (a) RPA and (b) DFT-PBE0 levels of approach.

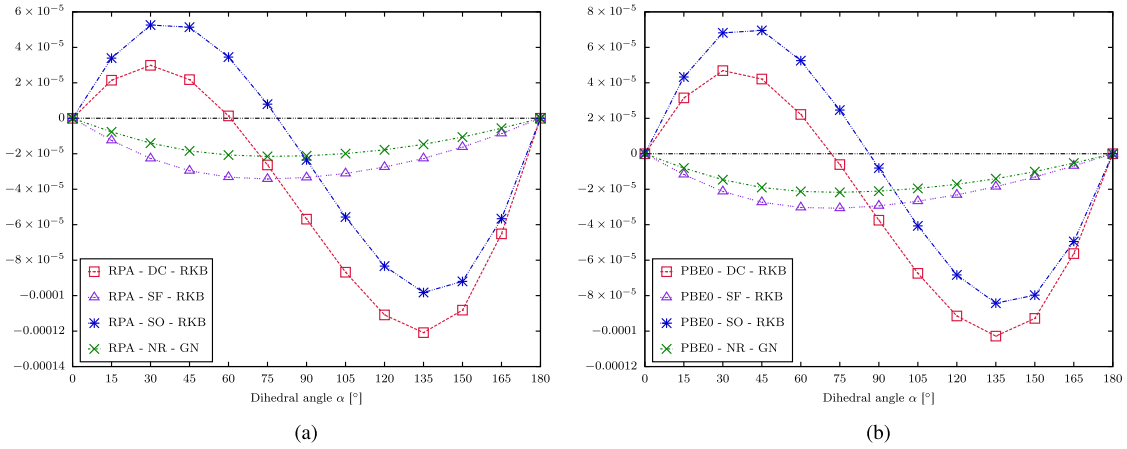

FIG. 7. Same as in Fig. 4, but for ^{125}Te in H_2Te_2 at the (a) RPA and (b) DFT-PBE0 levels of approach.

For a qualitative analysis of M_{iso}^{PV}, relativistic effects are not needed when ^{17}O and ^{33}S nuclei are studied. This is not the case for the nuclei belonging to the fourth row of the Periodic Table or the heaviest ones. In Figs. 6 and 7, it can be seen that for ^{77}Se and ^{125}Te, the SO effects are dependent on the dihedral angle α like a function $\sin(2\alpha)$, as in the case of their lightest homologous. For both selenium and tellurium nuclei, the relativistic effects are dominated by SO effects, and the inclusion of these effects is mandatory because they change the magnitude, the qualitative behavior, and even, for some dihedral angles, the sign of M_{iso}^{PV} (for the behavior of σ_{iso}^{PV}, see Figs. 1–3 of the supplementary material).

For the particular case of ^{209}Po in H_2Po_2, Fig. 8 shows that M_{iso}^{PV}(^{209}Po) has an almost purely relativistic nature. In other words, its NR limit is negligible compared with 4c calculations. Furthermore, the SO interactions are responsible for these effects, whereas the SF part is also negligible.

Table VII shows the scaling factor n (with respect to the atomic number Z) of the absolute value of the PV-NSR (isotropic) constants for nuclei X (X =^{33}S, ^{77}Se, ^{125}Te, and ^{209}Po) in H_2X_2 at a dihedral angle of 45°, taking results for the oxygen nucleus as reference. In

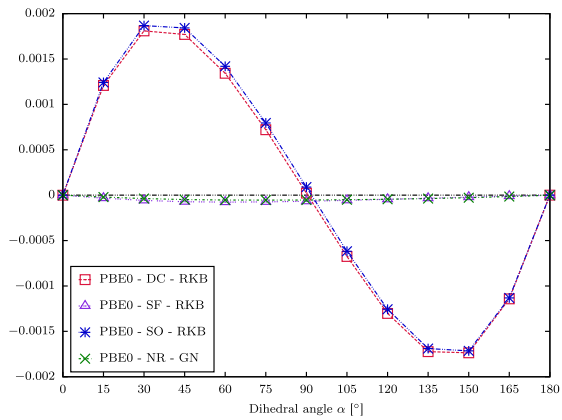

FIG. 8. Values of M_{iso}^{PV} (^{209}Po) for H_2Po_2 (in Hz) at different dihedral angles employing the DC, SF, and LL Hamiltonians at the DFT-PBE0 level of approach, employing the dyall.aae4z basis set. The SO contribution is the difference between DC and SF.

TABLE VII. Isotropic PV-NSR constants M_{iso}^{PV} (in Hz) of the X nuclei (X = ^{17}O, ^{33}S, ^{77}Se, ^{125}Te, and ^{209}Po) for P enantiomers of the H_2X_2 series of molecules at a dihedral angle of 45° and employing the dyall.aae4z basis set. Z_X is the atomic number of nucleus X. The values in parentheses are Z-scaling exponents n.

		$M_{iso}^{PV}(X)$	n	$M_{iso}^{PV}(X)$	n	$M_{iso}^{PV}(X)$	n	$M_{iso}^{PV}(X)$	n
Z_X	Method	DC (RKB)		SF (RKB)		SO (RKB)		NR (PN)	
8	RPA	-4.82×10^{-7}		-5.18×10^{-7}		3.54×10^{-8}		-5.18×10^{-7}	
	PBE0	-3.82×10^{-7}		-4.24×10^{-7}		4.14×10^{-8}		-4.27×10^{-7}	
16	RPA	-2.74×10^{-6}	(2.51)	-2.84×10^{-6}	(2.45)	9.75×10^{-8}	(1.46)	-2.69×10^{-6}	(2.38)
	PBE0	-2.88×10^{-6}	(2.91)	-2.99×10^{-6}	(2.82)	1.12×10^{-7}	(1.44)	-2.85×10^{-6}	(2.74)
34	RPA	-2.48×10^{-6}	(1.13)	-1.06×10^{-5}	(2.08)	8.09×10^{-6}	(3.75)	-8.62×10^{-6}	(1.94)
	PBE0	7.24×10^{-7}	(0.44)	-9.63×10^{-6}	(2.16)	1.04×10^{-5}	(3.82)	-8.27×10^{-6}	(2.05)
52	RPA	2.18×10^{-5}	(2.04)	-2.96×10^{-5}	(2.16)	5.14×10^{-5}	(3.89)	-1.84×10^{-5}	(1.91)
	PBE0	4.21×10^{-5}	(2.51)	-2.74×10^{-5}	(2.23)	6.95×10^{-5}	(3.97)	-1.91×10^{-5}	(2.03)
84	RPA	2.59×10^{-3}[a]	(3.65)[a]	-1.14×10^{-4}	(2.30)	2.71×10^{-3}[a]	(4.78)[a]	-4.64×10^{-5}	(1.91)
	PBE0	1.77×10^{-3}	(3.59)	-7.22×10^{-5}	(2.18)	1.85×10^{-3}	(4.55)	-4.83×10^{-5}	(2.01)

[a]Calculations with quasi-instabilities.

other words, n is calculated employing the relation

$$|M_{iso}^{PV}(X)| = |M_{iso}^{PV}(\mathrm{O})| \left(\frac{Z_X}{Z_\mathrm{O}}\right)^n. \quad (42)$$

It can be seen that the NR values scale as $Z^{2.32\pm0.42}$, with a similar behavior for to SF calculations whose scaling factor is $Z^{2.45\pm0.37}$. On the other hand, the SO contributions, which are responsible of most of the relativistic effects in M_{iso}^{PV}, scale as $Z^{2.99\pm1.56}$. The total four-component Dirac–Coulomb isotropic PV-NSR constant scales with $Z^{2.81\pm0.78}$ for all elements but selenium, where the DC results go from negative to positive values at a dihedral angle of about 45° and so the scaling factor should be analyzed with care for this molecule. We can thus conclude that the $Z^{3\pm1}$ scaling inferred in Ref. 23 for PV NMR shieldings is also satisfied for PV-NSR constants.

V. CONCLUSIONS

In this work, we have presented a four-component relativistic theory of the nuclear spin-dependent contribution to the PV-NSR tensor. By implementing this theory in the DIRAC code,[58] we have studied the influence of relativistic and electronic correlation effects on isotropic PV-NSR constants taking the H_2X_2 molecules as test systems (X = ^{17}O, ^{33}S, ^{77}Se, ^{125}Te, and ^{209}Po).

We calculated the SO and SF contributions to this property separately, as well as its NR limit. It was shown that for a dihedral angle of 45°, the SO contributions scale approximately as Z^4 for Se, Te, and Po (for sulfur, it scales as $Z^{1.5}$), whereas the SF contributions have a scaling behavior of Z^2 for all these nuclei. In addition, the SO and SF contributions are of opposite signs. As expected, the total effect of relativity increases with the increase in Z. For a dihedral angle of 45°, the relativistic effects go from 5% to 7% for oxygen, up to a difference of two orders of magnitude and change of sign for polonium. In addition, the SO contribution to M_{iso}^{PV}(^{209}Po) is between 23 and 26 times greater than its SF counterpart. The SO effects are important already for H_2Se_2 even from a qualitative point of view. They are responsible for the change in the sign of total M_{iso}^{PV}(^{77}Se) and also for the increase in its absolute value of up to three times, with respect to its NR limit. On the other hand, correlation contribution does not have a strong impact on the behavior of M_{iso}^{PV} with respect to the dihedral angle.

While the systems studied in this work are of minor interest from an experimental point of view, we provide an investigation of the expected size of the PV contributions to the NSR constants. We have found that for ^{209}Po in H_2Po_2, the PV-NSR contribution is of the order of 1 mHz. It is important to stress that parity-conserving isotropic NSR constants[29] are also very dependent on the inclusion of relativistic effects. In fact, the 4c-DC calculations of M_{iso}(^{209}Po) in H_2Po_2 at RPA, DFT-PBE0, and DFT-KT3 levels of theory give values between −280 and −160 kHz for the different dihedral angles, whereas their NR counterparts range between −140 and −120 kHz. These results give us the opportunity to compare the differences in the orders of magnitude of PV and parity-conserving contributions to the NSR (isotropic) constants. A natural extension of the work presented here is to search for promising molecules for measurements that are experimentally accessible and benefit from large PV-NSR contributions. We will use the insights from earlier works on PV-NMR-shielding[28,76–81] as a starting point to identify potential candidates for further computational investigations.

SUPPLEMENTARY MATERIAL

See the supplementary material for the complete set of calculations of PV-NSR and PV-NMR shieldings in the studied H_2X_2 (X = ^{17}O, ^{33}S, ^{77}Se, ^{125}Te, and ^{209}Po) molecules.

ACKNOWLEDGMENTS

I.A.A. acknowledges support from CONICET by Grant No. PIP 112-20130100361 and FONCYT by Grant No. PICT 2016-2936.

The authors acknowledge the Institute for Modeling and Innovation on Technologies (IMIT) of the National Scientific and Technical Research Council and Northeastern University of Argentina and also the Center for Information Technology of the University of Groningen for their support and for providing access to the IMIT and Peregrine high performance computing clusters.

AUTHOR DECLARATIONS

Conflict of Interest

The authors have no conflicts to disclose.

DATA AVAILABILITY

The data that support the findings of this study are available within the article and its supplementary material.

REFERENCES

[1] T. D. Lee and C. N. Yang, Phys. Rev. **104**, 254 (1956).
[2] C. S. Wu, E. Ambler, R. W. Hayward, D. D. Hoppes, and R. P. Hudson, Phys. Rev. **105**, 1413 (1957).
[3] M. Quack, Angew. Chem. **41**, 4618 (2002).
[4] R. Berger, in *Relativistic Electronic Structure Theory*, edited by P. Schwerdtfeger (Elsevier, 2004), Vol. 14, pp. 188–288.
[5] Y. B. Zel'dovich, D. Saakyan, and I. Sobel'man, JETP Lett. **25**, 94 (1977).
[6] M. A. Bouchiat and C. Bouchiat, J. Phys. France **35**, 899 (1974).
[7] C. S. Wood, S. C. Bennett, D. Cho, B. P. Masterson, J. L. Roberts, C. E. Tanner, and C. E. Wieman, Science **275**, 1759 (1997).
[8] L. M. Barkov and M. S. Zolotorev, Sov. Phys. JETP **52**, 360 (1980).
[9] R. Conti, P. Bucksbaum, S. Chu, E. Commins, and L. Hunter, Phys. Rev. Lett. **42**, 343 (1979).
[10] M. A. Bouchiat, J. Guéna, L. Hunter, and L. Pottier, Phys. Lett. B **117**, 358 (1982).
[11] T. P. Emmons, J. M. Reeves, and E. N. Fortson, Phys. Rev. Lett. **51**, 2089 (1983).
[12] M. J. D. Macpherson, K. P. Zetie, R. B. Warrington, D. N. Stacey, and J. P. Hoare, Phys. Rev. Lett. **67**, 2784 (1991).
[13] K. Tsigutkin, D. Dounas-Frazer, A. Family, J. E. Stalnaker, V. V. Yashchuk, and D. Budker, Phys. Rev. Lett. **103**, 071601 (2009).
[14] V. S. Letokhov, Phys. Lett. A **53**, 275 (1975).
[15] B. Darquié, C. Stoeffler, A. Shelkovnikov, C. Daussy, A. Amy-Klein, C. Chardonnet, S. Zrig, L. Guy, J. Crassous, P. Soulard, P. Asselin, T. R. Huet, P. Schwerdtfeger, R. Bast, and T. Saue, Chirality **22**, 870 (2010).
[16] F. Hobi, R. Berger, and J. Stohner, Mol. Phys. **111**, 2345 (2013).
[17] A. Cournol, M. Manceau, M. Pierens, L. Lecordier, D. B. A. Tran, R. Santagata, B. Argence, A. Goncharov, O. Lopez, M. Abgrall, Y. Le Coq, R. Le Targat, H. Alvarez Martinez, W. K. Lee, D. Xu, P. E. Pottie, R. J. Hendricks, T. E. Wall, J. M. Bieniewska, B. E. Sauer, M. R. Tarbutt, A. Amy-Klein, S. K. Tokunaga, and B. Darquié, Quantum Electron. **49**, 288 (2019).
[18] V. G. Gorshkov, M. G. Kozlov, and L. N. Labzovskii, Sov. Phys. JETP **55**, 1042 (1982).
[19] A. L. Barra, J. B. Robert, and L. Wiesenfeld, Phys. Lett. A **115**, 443 (1986).
[20] A. L. Barra, J. B. Robert, and L. Wiesenfeld, Europhys. Lett. **5**, 217 (1988).
[21] A. L. Barra and J. B. Robert, Mol. Phys. **88**, 875 (1996).
[22] A. Soncini, F. Faglioni, and P. Lazzeretti, Phys. Rev. A **68**, 033402 (2003).
[23] G. Laubender and R. Berger, ChemPhysChem **4**, 395 (2003).
[24] V. Weijo, P. Manninen, and J. Vaara, J. Chem. Phys. **123**, 054501 (2005).
[25] G. Laubender and R. Berger, Phys. Rev. A **74**, 032105 (2006).
[26] R. Bast, P. Schwerdtfeger, and T. Saue, J. Chem. Phys. **125**, 064504 (2006).
[27] S. Nahrwold and R. Berger, J. Chem. Phys. **130**, 214101 (2009).
[28] J. Eills, J. W. Blanchard, L. Bougas, M. G. Kozlov, A. Pines, and D. Budker, Phys. Rev. A **96**, 042119 (2017).
[29] I. A. Aucar, S. S. Gómez, M. C. Ruiz de Azúa, and C. G. Giribet, J. Chem. Phys. **136**, 204119 (2012).
[30] I. A. Aucar, S. S. Gómez, J. I. Melo, C. G. Giribet, and M. C. Ruiz de Azúa, J. Chem. Phys. **138**, 134107 (2013).
[31] G. A. Aucar and I. A. Aucar, in *Annual Reports on NMR Spectroscopy*, edited by G. A. Webb (Academic, San Diego, 2019), Vol. 96, pp. 77–141.
[32] Y. Xiao and W. Liu, J. Chem. Phys. **138**, 134104 (2013).
[33] E. Malkin, S. Komorovský, M. Repisky, T. B. Demissie, and K. Ruud, J. Phys. Chem. Lett. **4**, 459 (2013).
[34] S. Komorovský, M. Repisky, E. Malkin, T. B. Demissie, and K. Ruud, J. Chem. Theory Comput. **11**, 3729 (2015).
[35] J. K. Laerdahl and P. Schwerdtfeger, Phys. Rev. A **60**, 4439 (1999).
[36] R. Berger and M. Quack, J. Chem. Phys. **112**, 3148 (2000).
[37] V. Weijo, R. Bast, P. Manninen, T. Saue, and J. Vaara, J. Chem. Phys. **126**, 074107 (2007).
[38] J. Oddershede, in *Advances in Quantum Chemistry*, edited by P.-O. Löwdin (Academic, San Diego, 1978), Vol. 11, pp. 275–352.
[39] T. Helgaker, S. Coriani, P. Jørgensen, K. Kristensen, J. Olsen, and K. Ruud, Chem. Rev. **112**, 543 (2012).
[40] Y. Y. Rusakov and L. B. Krivdin, Russ. Chem. Rev. **82**, 99 (2013).
[41] G. A. Aucar, Phys. Chem. Chem. Phys. **16**, 4420 (2014).
[42] G. A. Aucar, R. H. Romero, and A. F. Maldonado, Int. Rev. Phys. Chem. **29**, 1 (2010).
[43] T. Saue and H. J. A. Jensen, J. Chem. Phys. **118**, 522 (2003).
[44] V. Flambaum and I. Khriplovich, Sov. Phys. JETP **52**, 835 (1980).
[45] S. A. Blundell, J. Sapirstein, and W. R. Johnson, Phys. Rev. D **45**, 1602 (1992).
[46] E. Tiesinga, P. J. Mohr, D. B. Newell, and B. N. Taylor, The 2018 CODATA Recommended Values of the Fundamental Physical Constants (Web Version 8.1), http://physics.nist.gov/constants, Database developed by J. Baker, M. Douma, and S. Kotochigova, National Institute of Standards and Technology, Gaithersburg, MD.
[47] P. A. Zyla *et al.* (Particle Data Group), Prog. Theor. Exp. Phys. **2020**, 083C01.
[48] L. Montanet, K. Gieselmann, R. M. Barnett, D. E. Groom, T. G. Trippe, C. G. Wohl, B. Armstrong, G. S. Wagman, H. Murayama, J. Stone, J. J. Hernandez, F. C. Porter, R. J. Morrison, A. Manohar, M. Aguilar-Benitez, C. Caso, P. Lantero, R. L. Crawford, M. Roos, N. A. Törnqvist, K. G. Hayes, G. Höhler, S. Kawabata, D. M. Manley, K. Olive, R. E. Shrock, S. Eidelman, R. H. Schindler, A. Gurtu, K. Hikasa, G. Conforto, R. L. Workman, and C. Grab (Particle Data Group), Phys. Rev. D **50**, 1173 (1994).
[49] V. V. Flambaum, I. B. Khriplovich, and O. P. Sushkov, Phys. Lett. B **146**, 367 (1984).
[50] I. A. Aucar, S. S. Gómez, C. G. Giribet, and M. C. Ruiz de Azúa, J. Chem. Phys. **139**, 094112 (2013).
[51] J. I. Melo, M. C. Ruiz de Azúa, C. G. Giribet, G. A. Aucar, and R. H. Romero, J. Chem. Phys. **118**, 471 (2003).
[52] G. A. Aucar, J. I. Melo, I. A. Aucar, and A. F. Maldonado, Int. J. Quantum Chem. **118**, e25487 (2018).
[53] I. A. Aucar, S. S. Gomez, C. G. Giribet, and M. C. Ruiz de Azúa, J. Chem. Phys. **141**, 194103 (2014).
[54] G. A. Aucar, T. Saue, L. Visscher, and H. J. A. Jensen, J. Chem. Phys. **110**, 6208 (1999).
[55] W. H. Flygare, J. Chem. Phys. **41**, 793 (1964).
[56] W. H. Flygare, Chem. Rev. **74**, 653 (1974).
[57] P. Raghavan, At. Data Nucl. Data Tables **42**, 189 (1989).
[58] Dirac, a relativistic *ab initio* electronic structure program, Release dirac19 (2019), written by A. S. P. Gomes, T. Saue, L. Visscher, H. J. Aa. Jensen, and R. Bast, with contributions from I. A. Aucar, V. Bakken, K. G. Dyall, S. Dubillard, U. Ekström, E. Eliav, T. Enevoldsen, E. Faßhauer, T. Fleig, O. Fossgaard, L. Halbert, E. D. Hedegård, B. Heimlich–Paris, T. Helgaker, J. Henriksson, M. Iliaš, Ch. R. Jacob, S. Knecht, S. Komorovský, O. Kullie, J. K. Lærdahl, C. V. Larsen, Y. S. Lee, H. S. Nataraj, M. K. Nayak, P. Norman, G. Olejniczak, J. Olsen, J. M. H. Olsen, Y. C. Park, J. K. Pedersen, M. Pernpointner, R. di Remigio, K. Ruud, P. Sałek, B. Schimmelpfennig, B. Senjean, A. Shee, J. Sikkema, A. J. Thorvaldsen, J. Thyssen, J. van Stralen, M. L. Vidal, S. Villaume, O. Visser, T. Winther, and S. Yamamoto, available at http://dx.doi.org/10.5281/zenodo.3572669, see also http://www.diracprogram.org.
[59] T. Saue, R. Bast, A. S. P. Gomes, H. J. A. Jensen, L. Visscher, I. A. Aucar, R. Di Remigio, K. G. Dyall, E. Eliav, E. Fasshauer, T. Fleig, L. Halbert, E. D. Hedegård, B. Helmich-Paris, M. Iliaš, C. R. Jacob, S. Knecht, J. K. Laerdahl, M. L. Vidal, M. K. Nayak, M. Olejniczak, J. M. H. Olsen, M. Pernpointner, B. Senjean, A. Shee, A. Sunaga, and J. N. P. van Stralen, J. Chem. Phys. **152**, 204104 (2020).
[60] K. G. Dyall, Theor. Chem. Acc. **135**, 128 (2016).
[61] K. G. Dyall, Theor. Chem. Acc. **99**, 366 (1998).

[62]K. G. Dyall, Theor. Chem. Acc. **108**, 365 (2002).
[63]K. G. Dyall, Theor. Chem. Acc. **115**, 441 (2006).
[64]K. G. Dyall, Theor. Chem. Acc. **131**, 1217 (2012).
[65]T. Saue, in *Advances in Quantum Chemistry*, edited by J. R. Sabin (Academic, San Diego, 2005), Vol. 48, pp. 383–405.
[66]L. Visscher, Theor Chem Acc **98**, 68–70 (1997).
[67]L. Visscher and K. G. Dyall, At. Data Nucl. Data Tables **67**, 207 (1997).
[68]T. W. Keal and D. J. Tozer, J. Chem. Phys. **121**, 5654 (2004).
[69]C. Adamo and V. Barone, J. Chem. Phys. **110**, 6158 (1999).
[70]I. A. Aucar, C. A. Giménez, and G. A. Aucar, RSC Adv. **8**, 20234 (2018).
[71]D. F. E. Bajac, I. A. Aucar, and G. A. Aucar, Phys. Rev. A **104**, 012805 (2021).
[72]T. H. Dunning, J. Chem. Phys. **90**, 1007 (1989).
[73]A. K. Wilson, D. E. Woon, K. A. Peterson, and T. H. Dunning, J. Chem. Phys. **110**, 7667 (1999).
[74]W. Kutzelnigg, Phys. Rev. A **67**, 032109 (2003).
[75]A. F. Maldonado and G. A. Aucar, Phys. Chem. Chem. Phys. **11**, 5615 (2009).
[76]R. Berger and J. L. Stuber, Mol. Phys. **105**, 41 (2007).
[77]R. Zanasi, S. Pelloni, and P. Lazzeretti, J. Comput. Chem. **28**, 2159 (2007).
[78]D. Figgen and P. Schwerdtfeger, Phys. Rev. A **78**, 012511 (2008).
[79]V. Weijo, P. Manninen, and J. Vaara, Theor. Chem. Acc. **121**, 53 (2008).
[80]V. Weijo, M. B. Hansen, O. Christiansen, and P. Manninen, Chem. Phys. Lett. **470**, 166 (2009).
[81]S. Nahrwold, R. Berger, and P. Schwerdtfeger, J. Chem. Phys. **140**, 024305 (2014).